https://doi.org/10.5194/egusphere-2025-990
Preprint. Discussion started: 22 April 2025

A novel method for correcting water budget components and reducing their uncertainties by optimally distributing the imbalance residual without full closure

Zengliang Luo[a,b], Hanjia Fu[a,b], Quanxi Shao[c]*, Wenwen Dong[a,b], Xi Chen[d], Xiangyi Ding[e]*, Lunche Wang[a,b], Xihui Gu[a,b], Ranjan Sarukkalige[f], Heqing Huang[a,b], Huan Li[g]

[a] Hubei Key Laboratory of Regional Ecology and Environmental Change, State Key Laboratory of Geomicrobiology and Environmental Changes, China University of Geosciences, Wuhan 430074, China.

[b] State Key Laboratory of Biogeology and Environmental Geology, China University of Geosciences, Wuhan 430074, China.

[c] CSIRO Data61, Australian Resources Research Centre, 26 Dick Perry Avenue, Kensington, WA 6155, Australia.

[d] State Key Laboratory of Remote Sensing Science, Aerospace Information Research Institute, Chinese Academy of Sciences, Beijing, 100101, China.

[e] Department of Water Resources, China Institute of Water Resources and Hydropower Research, Beijing 100038, China.

[f] School of Civil and Mechanical Engineering, Curtin University, GPO Box U1987, Perth, WA 6845, Australia.

[g] HUN-REN Balaton Limnological Research Institute, Hungary.

Corresponding author to: Quanxi Shao (Quanxi.Shao@data61.csiro.au) and Xiangyi Ding (dingxy@iwhr.com)

Highlights:

- There are around 5% (with range between 0 to 10%) of cases where errors introduced by current BCC methods are so large that some budget components become negative
- A Novel IWE-Res method is proposed to identify the optimal balance for redistributing ΔRes
- The optimal redistribution of ΔRes is found between 40%-90% in most basins, except for cold regions.

Abstracts: Closing the water budget improves the consistency of water budget component datasets, including precipitation (P), evapotranspiration (ET), streamflow

https://doi.org/10.5194/egusphere-2025-990
Preprint. Discussion started: 22 April 2025

(Q) and terrestrial water storage change (TWSC), thereby enhancing the understanding of basin-scale water cycle processes. Existing water budget closure correction (BCC) methods typically redistribute the entire water imbalance error (ΔRes) to achieve perfect water budget closure but often neglect the trade-off between achieving closure and the errors introduced into budget components as a result of this redistribution. This study quantifies the uncertainties introduced by existing BCC methods (CKF, MCL, MSD, and PR) across 84 basins representing diverse climate zones. We then propose a novel method, IWE-Res, to identify the optimal balance for redistributing ΔRes. This method minimizes the combined error from both introduced budget component errors and the remaining ΔRes error, while reducing the occurrence of negative values. The results indicate: (1) Existing BCC methods can lead to negative values in corrected budget components, with negative values comprising approximately 0–10% (mostly below 5%) of the time series; (2) Compared to existing BCC methods, the proposed IWE-Res method improves the accuracy of corrected P by 29.5%, corrected ET by 24.7%, corrected Q by 69.0%, and corrected TWSC by 6.8% based on the root mean square error (RMSE); and (3) In most basins, except in cold regions, the optimal balance is reached when 40%–90% of ΔRes is redistributed. By offering a more balanced approach to water budget closure, this study improves the accuracy and reliability of corrected budget component datasets.

Keywords: Water budget closure; Budget components; Water imbalance; Uncertainty identification; Global hydrology

https://doi.org/10.5194/egusphere-2025-990
Preprint. Discussion started: 22 April 2025

1 Introduction

Closing the water budget is essential for understanding water circulation among the atmosphere, surface, soil, and groundwater (Li et al., 2024; Mourad et al., 2024). However, the absence of integrated observational systems capable of measuring all water budget components simultaneously—since these components are typically observed separately—makes it challenging to obtain datasets that achieve water budget closure (Eq. 1) through direct observations (Zheng et al., 2025).

$$\mathrm{P} - \mathrm{ET} - \mathrm{Q} - \mathrm{TWSC} = 0 \tag{1}$$

where P represents precipitation, ET represents evapotranspiration, Q represents streamflow, and TWSC represents terrestrial water storage change.

In research and applications, hydrological models are designed based on the principle of water balance. However, extensive simplifications and error propagation within these models (arising from input data, model structure, and parameter uncertainties) introduce errors in the simulation of budget components, making water budget closure equally challenging. In the era of big data, the growing availability of remote sensing and reanalysis datasets offers greater potential for achieving water budget closure (Zhou et al., 2024). To correct water imbalance error (ΔRes) and ensure ΔRes = 0 (where ΔRes = P – ET – Q – TWSC), various water budget closure correction (BCC) methods have been proposed and widely adopted. Common methods include Proportional Redistribution (PR), the Constrained Kalman Filter (CKF), Multiple Collocation (MCL), and the Minimized Series Deviation (MSD) method (Pan et al., 2012; Luo et al., 2023). For example, Abhishek et al. (2021)

https://doi.org/10.5194/egusphere-2025-990
Preprint. Discussion started: 22 April 2025

applied the PR, CKF, and MCL methods to quantify water budget closure and uncertainties in budget components in the upper Chao Phraya River basin; Abolafia-Rosenzweig et al. (2021) evaluated the effectiveness of PR, CKF, and MCL methods in closing the water budget for 24 global basins; Dastjerdi et al. (2024) developed a precipitation data merging method to improve precipitation estimates based on existing BCC methods.

Existing BCC methods achieve water budget closure by redistributing the entire ΔRes error across budget components, with redistribution weights estimated based on errors in these components. However, ΔRes represents a composite error that includes not only inaccuracies in measured components but also contributions from unmeasured components. The latter is prevalent but difficult to attribute to specific budget components using existing technologies. Consequently, existing BCC methods determine redistribution weights solely based on estimated errors in budget components. Since existing BCC methods address only ΔRes errors arising from inaccuracies in measured components, they inherently conflict with the goal of achieving a fully closed water budget. This limitation explains why, despite aiming to improve the accuracy of P, ET, Q, and TWSC estimates through complete redistribution of ΔRes, existing BCC methods may lead to limited improvements—or even a decline—in the accuracy of corrected budget component datasets.

A clear manifestation of this issue is the occurrence of negative values in corrected budget component datasets, such as negative P, ET, and Q. Our previous work also found that enforcing water budget closure may, to some extent, reduce the

https://doi.org/10.5194/egusphere-2025-990
Preprint. Discussion started: 22 April 2025

accuracy of budget components and tends to introduce an ET regulation factor to mitigate accuracy loss in ET caused by existing BCC methods (Luo et al., 2023). A more effective approach to addressing this issue may involve identifying an optimal distribution of the ΔRes error that balances errors introduced in budget components with the remaining ΔRes error. Specifically, ΔRes errors arising from inaccuracies in budget components should be redistributed while preventing the negative values associated with existing BCC methods.

The key question we aim to answer in this study is the extent of uncertainty introduced into budget components by existing BCC methods for enforcing water budget closure and, more critically, whether this uncertainty exceeds the reduction in the ΔRes error. If the introduced uncertainty outweighs the error reduction, fully closing the water budget may be unnecessary. As noted earlier, ΔRes represents a composite error, whereas existing BCC methods primarily address errors in budget components. We propose that an optimal balance for redistributing the ΔRes error should be identified—one that minimizes the combined error from budget components and the remaining water imbalance. This optimal balance allows for redistributing only the portion of ΔRes attributable to errors in budget components, rather than the entire ΔRes, thereby preventing the occurrence of negative values in budget components due to improper error redistribution. However, research on identifying this optimal balance, which is crucial for improving existing BCC methods, remains lacking.

The primary objective of this study is to quantify the uncertainties introduced by

https://doi.org/10.5194/egusphere-2025-990
Preprint. Discussion started: 22 April 2025

existing BCC methods in closing the water budget from multiple perspectives and to propose a new IWE-Res method for identifying the optimal balance in ΔRes redistribution. To enhance the robustness of error analysis and validate the proposed IWE-Res method, we applied four existing BCC methods with varying principles and complexities (PR, CKF, MCL, and MSD) across 84 global basins with diverse climatic characteristics. The specific objectives of this study are:

(1) To quantify the uncertainties introduced into budget components by enforcing water budget closure using existing BCC methods from multiple perspectives, including uncertainties relative to observations, the occurrence of negative values in budget components, and deviations from the original budget component datasets. This analysis provides a more comprehensive understanding of the trade-offs between achieving water budget closure and the associated errors;

(2) To analyze in detail the occurrence of negative corrected values in budget components caused by existing BCC methods, including the proportion of negative values within the time series of each budget component and their spatial distribution under varying climatic conditions;

(3) To compare the reduction in ΔRes with the corresponding increase in budget component errors resulting from enforced water budget closure;

(4) To propose a new method (IWE-Res) for identifying the optimal balance in ΔRes redistribution, minimizing the combined error from both introduced budget component errors and the remaining ΔRes error. The accuracy and reliability of the proposed IWE-Res method were validated through comparisons with existing BCC

https://doi.org/10.5194/egusphere-2025-990
Preprint. Discussion started: 22 April 2025

methods (PR, CKF, MCL, MSD).

2 Study area and data

To robustly quantify the uncertainties introduced by existing BCC methods in closing the water budget and to assess the accuracy of the proposed IWE-Res method across different climate zones, multiple river basins worldwide were selected as study areas. In total, 84 basins (Fig. 1) were chosen based on the availability of streamflow observations from the GRDC for the period 2002–2020. To ensure data reliability, the proportion of missing data was kept below 10%, with missing values interpolated using a linear method. Notably, approximately 90% of the basins used in this study had less than 5% missing data.

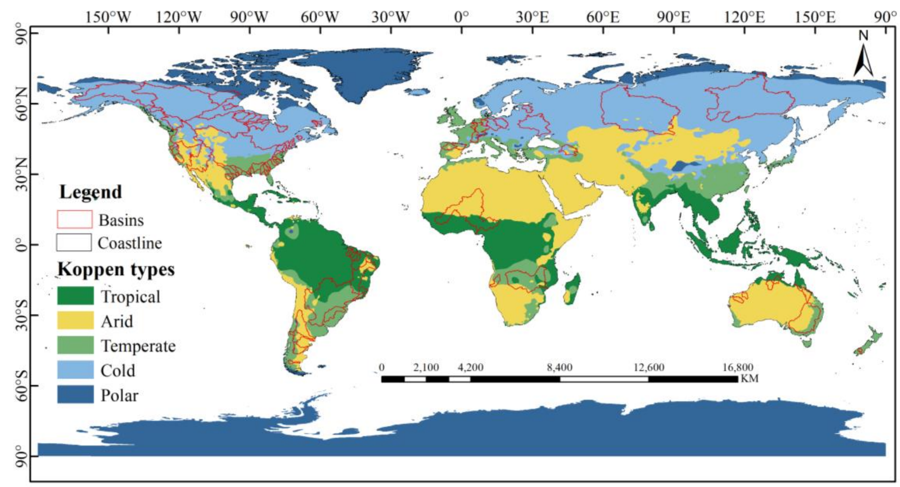

Fig. 1 Overview of the Study Area. The climate classification used in this study is based on the Köppen climate classification system.

The climate classifications presented in Fig. 1 were determined using the Köppen climate classification system, a widely adopted framework that categorizes global

https://doi.org/10.5194/egusphere-2025-990
Preprint. Discussion started: 22 April 2025

climates based on temperature and precipitation thresholds (Crosbie et al., 2012; Hansford et al., 2020; Liu et al., 2022; Papacharalampous et al., 2023). This system divides the world into five primary climate types—Tropical, Arid, Temperate, Cold, and Polar. Its key strength lies in its integration of climate data with vegetation distribution, making it highly relevant to ecological environments.

For each budget component, multiple datasets are typically available, with accuracy varying across different basins. No single dataset consistently performs best across all global basins. Therefore, multiple datasets were selected for each budget component to generate various data combinations (Equations 2–3). This approach ensures the inclusion of the most suitable dataset combinations while mitigating uncertainties associated with reliance on a single dataset.

In selecting datasets, priority was given to those incorporating extensive observational data, as they generally offer higher accuracy. We selected four P datasets—GPCC, GPM, MSWEP, and PERSIANN-CDR; three ET datasets—GLDAS, GLEAM, and TerraClimate; and three TWSC datasets derived from GRACE satellite observations—GRACE CSR, GRACE GFZ, and GRACE JPL. Observed Q data were obtained from the GRDC platform. By combining these datasets, a total of 36 distinct data combinations were generated for each basin (Equation 3).

$$\mathrm{Cjkl} = \left[P_j \;\; ET_k \;\; TWSC_l \;\; Q\right] \tag{2}$$

where j, k, and l represent the indices of the datasets corresponding to each budget component. Table 1 provides basic information on the datasets used in this study, along with their corresponding indices. Equation 3 represents a matrix composed of

https://doi.org/10.5194/egusphere-2025-990
Preprint. Discussion started: 22 April 2025

the elements defined in Equation 2.

$$C = \begin{bmatrix} C111 & C112 & C113 & C121 & C122 & C123 & C131 & C132 & C133 \\ C211 & C212 & C213 & C221 & C222 & C223 & C231 & C232 & C233 \\ C311 & C312 & C313 & C321 & C322 & C323 & C331 & C332 & C333 \\ C411 & C412 & C413 & C421 & C422 & C423 & C431 & C432 & C433 \end{bmatrix} \quad (3)$$

The Global Precipitation Climatology Centre (GPCC) dataset, operated and provided by the German Weather Service (DWD), is a global precipitation dataset based on ground station observations (Becker et al., 2013; Schneider et al., 2008). This dataset is generated through the quality control, spatial interpolation, and aggregation of observational data from various sources, resulting in a consistent, globally comprehensive precipitation product. It features a spatial resolution of 0.25° and is available at both daily and monthly time scales. The Global Precipitation Measurement Integrated Multi-Satellite Retrievals (GPM IMERG) dataset, initiated by NASA and JAXA, provides global precipitation estimates by integrating satellite sensor data with ground-based rain gauge observations and other auxiliary data, ensuring thorough calibration. The Multi-Source Weighted-Ensemble Precipitation (MSWEP) dataset is produced by optimally combining precipitation data from satellite observations, ground stations, and reanalysis products. It applies different weighting strategies across varying spatial and temporal scales to maximize data accuracy (Beck, Pan, et al., 2019; Beck et al., 2017; Beck, Wood, et al., 2019). The PERSIANN-CDR dataset, derived from satellite remote sensing and artificial neural network technology, covers latitudes from 60°S to 60°N, with a spatial resolution of 0.25° and daily temporal resolution.

The Global Land Data Assimilation System (GLDAS), jointly developed by

NASA and NOAA, employs advanced land surface modeling and data assimilation techniques to integrate satellite and ground-based observations, generating optimal fields of land surface states and fluxes. The GLDAS dataset has provided continuous global evapotranspiration data since 2000. The GLEAM evapotranspiration dataset, developed by the Miralles team at the University of Bristol, estimates global surface evapotranspiration using multi-satellite remote sensing data and the Priestley-Taylor retrieval algorithm. Potential evaporation is calculated based on observations of surface net radiation and near-surface air temperature. The potential evapotranspiration estimates are converted to actual evapotranspiration using a multiplicative evaporative stress factor, derived from microwave-based Vegetation Optical Depth (VOD) and root zone soil moisture estimates. TerraClimate utilizes the Penman-Monteith equation to estimate both global potential and actual evapotranspiration. To improve accuracy, TerraClimate’s evapotranspiration estimates are calibrated against ground-based observations and other climate data products, ensuring applicability across various climate regions and seasons (Abatzoglou et al., 2018).

The launch of gravity satellites has provided new opportunities for more accurate observations of large-scale TWSC in river basins. The Gravity Recovery and Climate Experiment (GRACE) was launched in March 2002 and completed its mission in November 2017. Its successor, GRACE Follow-On (GRACE-FO), was launched in May 2018, continuing the monitoring of Earth's gravity field and its changes (Boergens et al., 2024). The principle behind observing TWSC is the assumption that

https://doi.org/10.5194/egusphere-2025-990
Preprint. Discussion started: 22 April 2025

variations in terrestrial gravity are primarily caused by water mass changes. By tracking fluctuations in Earth's gravity field, information on the distribution and changes in surface water can be inferred. The GRACE TWSC datasets used in this study are provided by the University of Texas Center for Space Research (CSR), the German Research Centre for Geosciences (GFZ), and NASA’s Jet Propulsion Laboratory (JPL).

The Global Runoff Data Centre (GRDC) provides the most comprehensive open-access river discharge data available worldwide, collected from national hydrological agencies. This dataset includes river streamflow measurements from over 10,000 stations across 159 countries (Su et al., 2024). To minimize the impact of missing data on the reliability of the results, hydrological stations were selected based on the criterion that missing values accounted for less than 10% of the total dataset. Linear interpolation was then applied to fill any remaining data gaps.

Table 1 Datasets used for this study.

Variable	Data Source	Number	Resolution	Reference
P	Global Precipitation Climatology Centre (GPCC)	1	0.25°/month	Schneider et al. (2008)
	Global Precipitation Measurement (GPM)	2	0.1°/month	Huffman et al. (2015)
	Multi-Source Weighted-Ensemble Precipitation (MSWEP)	3	0.1°/month	Beck, Wood, et al. (2019)
	Precipitation Estimation from Remotely Sensed Information using Artificial Neural Networks — Climate Data Record (PERSIANN-CDR)	4	0.25°/month	Hsu et al. (1997)
ET	global land data assimilation system (GLDAS)	1	0.25°/month	Park and Choi (2015)
	Global Land Evaporation Amsterdam Model (GLEAM)	2	0.25°/month	Miralles et al. (2011)

https://doi.org/10.5194/egusphere-2025-990
Preprint. Discussion started: 22 April 2025

	TerraClimate	3	1/24°/month	Abatzoglou et al. (2018)
TWSC	Gravity Recovery and Climate Experiment (GRACE CSR)	1	1.0°/month	Watkins et al. (2015)
	Gravity Recovery and Climate Experiment (GRACE GFZ)	2	1.0°/month	Watkins et al. (2015)
	Gravity Recovery and Climate Experiment (GRACE JPL)	3	1.0°/month	Watkins et al. (2015)
Q	Global Runoff Data Centre (GRDC)	-	-	Burek and Smilovic (2022)

3 Methods

3.1 Water imbalance error

The water balance equation describes the conservation of mass between water inflows, outflows, and changes in storage within a given region (Equation 1). However, due to measurement errors, model simplifications, and unmeasured components (omissions), the observed budget components contain errors (named as ε_{P}, ε_{ET}, ε_{Q}, ε_{TWSC}, respectively), causing the water balance to be unclosed (Equation 1 becomes Equation 4) (Aires, 2014; Wong et al., 2021). The imbalance resulting from these errors is defined as the ΔRes error (Equation 5), representing inconsistencies among budget components.

Minimizing the ΔRes error is a key objective in practical hydrological applications, as it enhances the accuracy and reliability of budget component datasets. However, it is important to note that smaller ΔRes values may arise from error compensation among budget components rather than genuine improvements in data accuracy. Therefore, a high-precision water balance dataset is characterized not only by a near-zero ΔRes error but also by budget components that closely approximate their true values (Luo et al., 2021).

$$(\mathrm{P} + \varepsilon_P) - (\mathrm{ET} + \varepsilon_{ET}) - \left(\mathrm{Q} + \varepsilon_Q\right) - (\mathrm{TWSC} + \varepsilon_{TWSC}) = 0 \quad (4)$$

$$\Delta\mathrm{Res} = \varepsilon_{ET} + \varepsilon_Q + \varepsilon_{TWSC} - \varepsilon_P = P - ET - Q - TWSC \quad (5)$$

where ε_P, ε_{ET}, ε_Q, ε_{TWSC} are the errors in budget components of P, ET, Q, and TWSC relative to their true values, respectively.

3.2 Existing water budget closure correction methods

To minimize the ΔRes error in Equation 5 (reducing ΔRes from ≠0 to 0), various statistical BCC methods have been developed. These methods differ in their principles to redistributing the ΔRes error, leading to varying levels of introduced uncertainty. To systematically assess the uncertainties associated with existing BCC methods in closing the water budget and to reduce uncertainty in method selection, we evaluated four representative methods: PR, CKF, MCL, and MSD (Luo et al., 2023; Abolafia-Rosenzweig et al., 2021; Dastjerdi et al., 2024).

For each basin, these four methods were applied to 36 different data combinations (Equation 3), yielding 144 uncertainty estimates. The optimal combinations were identified using a 5% threshold. By averaging the errors introduced into budget components across these selected optimal combinations, we quantified the uncertainty associated with existing BCC methods. This approach minimizes uncertainties arising from both BCC method selection and budget component data selection, enabling a more objective evaluation of the errors introduced by existing BCC methods. A brief overview of the four BCC methods is provided below:

https://doi.org/10.5194/egusphere-2025-990
Preprint. Discussion started: 22 April 2025

(1) PR method

The PR method assumes that the error in budget components is proportional to their magnitudes (Abatzoglou et al., 2018). Based on the relative magnitudes of these variables, the ΔRes error is redistributed across them to achieve water budget closure (Equation 6).

$$F_i = X_i - \Delta Res(G_i)\left(\frac{|X_i|}{\sum_{j=1}^{n}|X_j|}\right) \tag{6}$$

where F_i and X_i represent the corrected and original data for budget components (P, ET, Q and TWSC), respectively; n denotes the number of budget components involved in the water budget closure calculation; ΔRes represents the water imbalance error; G is a constant vector defined as $G = [1\ -1\ -1\ -1]$.

(2) CKF method

The CKF method is developed based on the Kalman filter. For a given set of estimated budget components $X = [P\,ET\,Q\,TWSC]^T$ and their estimated errors $\Delta Res = GX \neq 0$ (where G is a constant vector, $G = [1\ -1\ -1\ -1]$), the goal is to find a new set of estimates $F = [P'\,ET'\,Q'\,TWSC']^T$ such that $GX' = 0$, achieving water budget closure (Pan et al., 2012). In simple terms, the CKF method redistributes the ΔRes among the budget components based on the error covariance of X, defined as $\Delta\varepsilon_{XX}$ (Equation 7), to obtain a closured dataset (Equation 9).

$$\Delta\varepsilon_{XX} = \overline{(X - X_0)(X - X_0)^T} \tag{7}$$

$$\Delta\varepsilon_{XX} = \begin{bmatrix} \Delta\varepsilon_{P-P} & \Delta\varepsilon_{P-ET} & \Delta\varepsilon_{P-Q} & \Delta\varepsilon_{P-TWSC} \\ \Delta\varepsilon_{ET-P} & \Delta\varepsilon_{ET-ET} & \Delta\varepsilon_{ET-Q} & \Delta\varepsilon_{ET-TWSC} \\ \Delta\varepsilon_{Q-P} & \Delta\varepsilon_{Q-ET} & \Delta\varepsilon_{Q-Q} & \Delta\varepsilon_{Q-TWSC} \\ \Delta\varepsilon_{TWSC-P} & \Delta\varepsilon_{TWSC-ET} & \Delta\varepsilon_{TWSC-Q} & \Delta\varepsilon_{TWSC-TWSC} \end{bmatrix} \tag{8}$$

where X_0 refers to the reference values of the estimated budget component. The

https://doi.org/10.5194/egusphere-2025-990
Preprint. Discussion started: 22 April 2025

dimension of $\Delta\varepsilon_{XX}$ is 4×4, representing the covariance of errors among the budget components (Equation 8).

$$F = X + K(0 - GX) \tag{9}$$

where $\mathrm{K} = \Delta\varepsilon_{XX}C^T(C\Delta\varepsilon_{XX}C^T)^{-1}$ is the Kalman gain. Setting $\mathrm{C}\hat{X} = \widehat{\Delta Res}$, and Equation 9 can be rewritten as Equation 10.

$$F = X - \Delta\varepsilon_{XX}G^T(G\Delta\varepsilon_{XX}G^T)^{-1}\Delta Res \tag{10}$$

(3) MCL method

The MCL method is an extension of the triple collocation (TC) method. It calculates the weights for redistributing the ΔRes error among budget components by estimating the errors relative to their true values (expressed as distances, without requiring knowledge of the true values). The fundamental equations of the MCL method are shown in Equations 11-12.

$$F_i = X_i - \Delta Res(G^i)(d^i_{xx_0-norm}) \tag{11}$$

$$d^i_{xx_0-norm} = \frac{d^i_{xx_0}}{\sum_{j=1}^{4}\left|d^j_{xx_0}\right|} \tag{12}$$

In these equations, F_i represents the corrected data for the i-th budget component; X_i denotes the original data for the i-th budget component; ΔRes represents the water imbalance error; $d^i_{xx_0-norm}$ represents the weight assigned to the i-th budget component, and $d^i_{xx_0}$ represents the distance between the i-th budget component and the true value, as calculated using the Monte Carlo (MC) method. For example, in the case of five precipitation data products ($N = 5$), the calculation of $d^i_{xx_0}$ ($d1t$, $d2t$, $d3t$, $d4t$, and $d5t$) is shown in Equations 13-14.

$$A_{(N)}y_{(N)} = b_{(N)} \tag{13}$$

https://doi.org/10.5194/egusphere-2025-990
Preprint. Discussion started: 22 April 2025

$$A_{(5)}=\begin{bmatrix}1&1&0&0&0\\1&0&1&0&0\\1&0&0&1&0\\1&0&0&0&1\\0&1&1&0&0\\0&1&0&1&0\\0&1&0&0&1\\0&0&1&1&0\\0&0&1&0&1\\0&0&0&1&1\end{bmatrix},\ y_{(5)}=\begin{bmatrix}d_{1t}^2\\d_{2t}^2\\d_{3t}^2\\d_{4t}^2\\d_{5t}^2\end{bmatrix},\ b_{(5)}=\begin{bmatrix}d_{12}^2\\d_{13}^2\\d_{14}^2\\d_{15}^2\\d_{23}^2\\d_{24}^2\\d_{25}^2\\d_{34}^2\\d_{35}^2\\d_{45}^2\end{bmatrix} \tag{14}$$

(4) MSD method

The MSD method redistributes the ΔRes to each budget component based on minimizing the time-series deviation error, aiming to reduce model uncertainties caused by errors in estimating time-point deviations (Luo et al., 2023). Specifically, the MSD method first calculates the minimum time-series deviation distance between remote sensing data for budget components and multi-source integrated data products (EO) (Equation 15).

$$D_{x,\to n}=-\frac{\left[\sum_{j=1}^{n}\left(y_{(EO,j)}-\overline{y_{(EO,\to n)}}\right)\left(x_{(RS,j)}-\overline{x_{(RS,\to n)}}\right)\right]^2}{\sum_{j=1}^{n}\left(x_{(RS,j)}-\overline{x_{(RS,\to n)}}\right)^2}+\sum_{j=1}^{n}\left(y_{(EO,j)}-\overline{y_{(EO,\to n)}}\right)^2 \tag{15}$$

where $D_{x,\to n}$ represents the minimum time-series deviation distance for budget component x (e.g., P, ET, TWSC); $y_{(EO,j)}$ and $x_{(RS,j)}$ refer to the integrated value and raw value of the budget component x, respectively; $\overline{y_{(EO,\to n)}}$ and $\overline{x_{(RS,\to n)}}$ denote the average deviation of budget component x from the first to the n-th time point.

Next, the MSD method calculates the weights for each budget component based on $D_{x,\to n}$ (Equation 16).

https://doi.org/10.5194/egusphere-2025-990
Preprint. Discussion started: 22 April 2025

$$w_{x,j} = \frac{D_{x,\rightarrow j}}{\sum_{i=1}^{4} D_{i,\rightarrow j}} \tag{16}$$

where $w_{x,j}$ is the weight of budget component x at time point j.

Finally, the weight calculation results from Equation 16 are substituted into Equation 17 to achieve water budget closure.

$$\begin{bmatrix} F_{P,j}^{BCC} \\ F_{ET,j}^{BCC} \\ F_{R,j}^{BCC} \\ F_{TWSC,j}^{BCC} \end{bmatrix} = \begin{bmatrix} F_{P,j}^{Raw} \\ F_{ET,j}^{Raw} \\ F_{R,j}^{Raw} \\ F_{TWSC,j}^{Raw} \end{bmatrix} - \Delta Res \begin{bmatrix} 1 \\ -1 \\ -1 \\ -1 \end{bmatrix} \begin{bmatrix} w_{P,j} \\ w_{ET,j} \\ w_{R,j} \\ w_{TWSC,j} \end{bmatrix} \tag{17}$$

where F^{BCC} represents the budget components (P, ET, Q, and TWSC) corrected for water budget closure, while F^{Raw} denotes the raw, uncorrected values of the budget components.

3.3 Uncertainties introduced by existing BCC methods for closing water budget

When the existing BCC methods described in Section 3.2 are applied to close the water budget, they redistribute ΔRes based on the estimated errors of budget components but neglect unmeasured components. This inevitably leads to an unreasonable redistribution of the ΔRes error, introducing new uncertainties. The magnitude of these introduced errors and whether they can be ignored remain unresolved, primarily due to insufficient observational data for some budget components, making it difficult to quantify the associated uncertainties.

Our analysis in this study reveals that when existing BCC methods are used for water budget closure, certain budget components that typically have positive values, such as P, ET, and Q, occasionally become negative in some months. Previous studies have also mentioned this issue (Lehmann et al., 2022). This clearly indicates an unreasonable redistribution of ΔRes errors, underscoring the urgent need for

https://doi.org/10.5194/egusphere-2025-990
Preprint. Discussion started: 22 April 2025

methodological improvements. Despite this issue, research on negative values remains limited. Key questions persist regarding the proportion of negative values in each budget component under current BCC methods, which variables are most susceptible to severe negative values, and how these errors vary throughout the year. Addressing these questions is critical for refining existing BCC methods.

Notably, quantifying negative values does not require observational data. To comprehensively assess the uncertainties introduced by forced water budget closure, we consider three aspects: errors of individual budget components relative to observed values (Section 4.2.1), negative values arising from budget closure (Section 4.2.2), and ensemble errors (Section 4.2.3).

(1) Errors of individual budget components

Quantifying this type of error requires determining reference values for budget components. However, for certain variables, such as ET, observational data are insufficient across global watersheds, posing a major challenge in accurately characterizing global ET patterns. As a result, approximate reference values must be used to ensure the reliability of the results.

In this study, reference values for budget components were established based on the following principles. For Q, long-term observational records from hydrological stations were available for all selected basins, meeting the study’s requirements. For TWSC, we utilized three observational datasets from the GRACE satellite, which currently provides the only large-scale measurements of basin water storage changes under rigorous quality control. The reliability of GRACE data has been validated

https://doi.org/10.5194/egusphere-2025-990
Preprint. Discussion started: 22 April 2025

through ground-based observations (Famiglietti et al., 2011; Landerer et al., 2020; Rodell et al., 2009; Tapley et al., 2004; Yeh et al., 2006). Thus, GRACE TWSC data can be considered approximately reliable. To further enhance its accuracy, we applied data fusion techniques, as described in Equation 18, to merge the three GRACE TWSC products into a single reference dataset (Munier & Aires, 2018; Zhang et al., 2018).

The uncertainty introduced by existing BCC methods for precipitation was evaluated from two perspectives. First, 13 basins with sufficient observational precipitation data were selected, using observed precipitation as the reference. This sample size was sufficient for assessing the uncertainties associated with existing BCC methods. Second, 71 additional basins lacking sufficient observational precipitation data were included, for which fused precipitation values, derived using Equation 18, served as reference. This approach enabled cross-validation of the reliability of the fused dataset by comparing results with those from basins with observational data, allowing the study to be extended to a larger number of basins.

ET is the most challenging budget component to measure directly. The scarcity of globally available ET observational data precludes the direct use of observed ET as a reference. To address this limitation, previous studies have either focused on a few basins with available observational data or compared multiple existing ET datasets. ET products are generally considered reliable if their magnitudes and trends align with those of other datasets (Chen et al., 2021; Pan et al., 2020; Xu et al., 2019). Some studies have also employed the fusion of multiple data products as a reference for ET

https://doi.org/10.5194/egusphere-2025-990
Preprint. Discussion started: 22 April 2025

validation (Jiménez et al., 2018; Mueller et al., 2011; Yao et al., 2014). Following this approach, we assessed the uncertainty introduced by existing BCC methods for ET by utilizing a fusion-based reference dataset.

$$\overline{M_x} = \sum_{i=1}^{n} M_{x,i} * \omega_i \ \ and\ \ \omega_i = \frac{1}{\sigma_i^2} / \sum_{i=1}^{1} \frac{1}{\sigma_i^2} \tag{18}$$

where $\overline{M_x}$ represents the fused value of the budget component, $M_{x,i}$ denotes the i-th product of the budget component; ω_i denotes the weight of the i-th product, and σ_i^2 refers to the covariance error of the i-th product, n is the total number of budget components, and x refers to P, ET or TWSC.

After establishing reference values for budget components, we quantify errors in the original data relative to these references, using the positive metric CC and inverse metric RMSE as examples, denoted as CC_1 and $RMSE_1$, respectively. Similarly, errors in the BCC-corrected data relative to the reference values are calculated, represented as CC_2 and $RMSE_2$.

To assess the uncertainties introduced by water budget closure, changes in CC and RMSE (CC′ and RMSE′) are computed using Equations 19 and 22. Positive values of CC′ and RMSE′ indicate an improvement in data accuracy following BCC correction, whereas negative values suggest a decline. In addition to CC and RMSE, other statistical metrics used in this study include the positive indicator NSE and the negative indicator MAE.

$$\mathrm{CC}' = CC_2 - CC_1 \tag{19}$$

$$NSE' = NSE_2 - NSE_1 \tag{20}$$

$$MAE' = MAE_1 - MAE_2 \tag{21}$$

https://doi.org/10.5194/egusphere-2025-990
Preprint. Discussion started: 22 April 2025

$$RMSE' = RMSE_1 - RMSE_2 \tag{22}$$

$$CC = \frac{\sum_{i=1}^{n}(Obs_i - \overline{Obs})(Sim_i - \overline{Sim})}{\sqrt{\sum_{i=1}^{n}(Obs_i - \overline{Obs})^2}\sqrt{\sum_{i=1}^{n}(Sim_i - \overline{Sim})^2}} \tag{23}$$

$$NSE = 1 - \frac{\sum_{i=1}^{n}(Sim_i - Obs_i)^2}{\sum_{i=1}^{n}(Obs_i - \overline{Obs})^2} \tag{24}$$

$$MAE = \frac{1}{n}\sum_{i=1}^{n}|Sim_i - Obs_i| \tag{25}$$

$$RMSE = \sqrt{\frac{1}{n}\sum_{i=1}^{n}(Obs_i - Sim_i)^2} \tag{26}$$

where Obs_i represents the reference value at time i, and Sim_i represents either the original data or the BCC-corrected data. $\overline{\mathrm{Obs}}$ and $\overline{Sim}$ represent the mean values of Obs and Sim, respectively, and n is the sample size.

(2) Negative values

Negative values are defined as the issue that arises when the BCC method is used to close the water budget, and the redistributed ΔRes error exceeds the actual values of budget components (P, ET, Q, and TWSC), causing P, ET, and Q to become negative. For TWSC, a negative value occurs when the corrected TWSC has an opposite sign to its raw value. These negative values represent only a subset of the errors introduced during water budget closure but reflect an extreme case of unreasonable ΔRes error redistribution, serving as an indicator of the BCC method's effectiveness.

When a budget component exhibits a negative value, the redistribution of ΔRes errors to other components is significantly affected, reducing the overall accuracy of the corrected datasets. Thus, negative values are a critical factor influencing the performance of existing BCC methods and should be prioritized for improvement. To better understand this issue, we analyze the proportion of negative values for each

https://doi.org/10.5194/egusphere-2025-990
Preprint. Discussion started: 22 April 2025

budget component, their seasonal distribution, and their sensitivity to climatic conditions (i.e., their prevalence in arid versus humid basins). Insights from this analysis were incorporated into the proposed IWE-Res method to address the occurrence of negative values (Section 3.4).

(3) Ensembled error of four budget components

The aforementioned evaluations (1) and (2) assess errors for individual budget components. To gain a more comprehensive understanding of the uncertainties introduced by water budget closure, we also evaluate the combined error. First, the absolute error (AE) of each budget component is calculated (using P as an example, see Equation 29). Second, the relative absolute error (RAE) is determined for each budget component (Equation 28). Finally, by aggregating the relative errors of individual components, we define the ensembled relative error (Equation 27) to quantify the overall error introduced by BCC methods.

$$F(Re)=\frac{1}{n}\sum_{i=1}^{n}\frac{|AE(P')|-|AE(P_{Raw})|+|AE(ET')|-|AE(ET_{Raw})|+|AE(Q')|-|AE(Q_{Raw})|+|AE(TWSC')|-|AE(TWSC_{Raw})|}{P_0+ET_0+Q_0+|TWSC_0|} \\ =\frac{1}{n}\sum_{i=1}^{n}\frac{RAE(P)+RAE(ET)+RAE(Q)+RAE(TWSC)}{P_0+ET_0+Q_0+|TWSC_0|} \tag{27}$$

$$RAE(P)=|AE(P')|-|AE(P_{Raw})| \tag{28}$$

$$AE(P)=|P-P_0| \tag{29}$$

where, $F(Re)$ represents the ensembled relative error, and RAE refers to the relative value of absolute error, with i denoting the month. The subscript "Raw" corresponds to the raw data of the budget components, the subscript 0 represents the observed data, the superscript “′” denotes the BCC-corrected data for the budget components. The degree of alteration induced by the BCC methods for each budget component are defined based on the value of $F(Re)$, and four intervals are established in 5% increments: no significant change [0-5%], minor change (5-10%], moderate change (10-15%], and significant change (>15%).

3.4 Proposed IWE-Res method for closing water budget

In this section, the IWE-Res method is proposed to identify the optimal balance for redistributing ΔRes, minimizing the sum of the introduced error to budget components and the remaining ΔRes error while reducing the negative values introduced by closing the water budget. The principle of the proposed IWE-Res method involves gradually redistributing portions of ΔRes to budget components in fixed percentage increments using existing BCC methods until an optimal balance is achieved. This balance minimizes the combined error resulting from the introduced error to budget components and the remaining ΔRes error. Gradual redistribution of ΔRes begins at 0%, with iterations designed to incrementally redistribute portions of ΔRes to the budget components. If negative values are identified in budget components during the iterations, further redistribution to the affected budget component will be suspended. Instead, in subsequent iterations, the remaining ΔRes error will be redistributed among the other budget components. The specific steps of the proposed IWE-Res method are as follows:

First, the ΔRes error is calculated using Equation 5 and the original datasets of budget components.

Second, an iterative loop is constructed to compute the errors introduced into budget components during the gradual redistribution of the ΔRes error and to address

https://doi.org/10.5194/egusphere-2025-990
Preprint. Discussion started: 22 April 2025

negative values. To more accurately identify the optimal balance, a step size of 0.1% of ΔRes is used in each iteration in this study. We denote the ΔRes redistributed to budget components in each iteration as x, where x∈[0, ΔRes].

During each redistribution of ΔRes, two error terms are computed: (1) the remaining ΔRes error, defined as ΔRes* = ΔRes − x, and (2) the error introduced to budget components due to the redistribution of the x error, denoted as IWE (Equation 31). When these errors are plotted in a coordinate system, two distinct curves emerge (Fig. 2), each representing a different error relationship. For ΔRes* (Equation 30), Figure 2 shows a fixed, monotonically decreasing linear trend, as 0.1% increments of ΔRes are uniformly redistributed to budget components using existing BCC methods. In contrast, the IWE curve exhibits a non-fixed shape, reflecting the cumulative error introduced to budget components during the redistribution of a portion of ΔRes (Equations 31–32). This variability in the IWE curve arises from the nonlinear relationship between the introduced budget component errors and the reduction in ΔRes error.

$$\Delta\mathrm{Res}^{*}=\mathrm{a}x+\mathrm{b}=-x+\Delta\mathrm{Res} \tag{30}$$

$$\mathrm{IWE}=\mathrm{F}(\varepsilon_{\mathrm{P}}, \varepsilon_{\mathrm{ET}}, \varepsilon_{\mathrm{Q}}, \varepsilon_{\mathrm{TWSC}})=\mathrm{F}(x, \mathrm{RAE}) \tag{31}$$

$$RAE=\frac{1}{4}\sum_{i=1}^{4}(RAE(P)+RAE(ET)+RAE(Q)+RAE(TWSC)) \tag{32}$$

where x represents the portion of ΔRes redistributed to the budget components, with a range from 0 to ΔRes. The terms ε_{P}, $\varepsilon_{\mathrm{ET}}$, ε_{Q}, $\varepsilon_{\mathrm{TWSC}}$ represent the errors introduced to P, ET, Q and TWSC, respectively, due to the redistribution of x to the budget components. F(x, RAE) denotes the RAE error calculated by the redistribution of the x

https://doi.org/10.5194/egusphere-2025-990
Preprint. Discussion started: 22 April 2025

error to budget components.

If negative values occur in certain budget components during the iterative process, the redistribution of water imbalance error to the budget component with negative values will be halted. In subsequent iterations, the weights for redistributing the water imbalance error will be recalculated, ensuring that the remaining budget components with positive values receive the redistributed water imbalance error. For instance, if one of the four budget components (P, ET, Q, and TWSC) produces a negative value—such as ET in a given iteration—the imbalance error for that iteration will be redistributed to P, Q, and TWSC according to Equation 33.

$$F_i = X_i - x(G_i)\left(\frac{|\varepsilon_i|}{\sum_{j=1}^{n}|\varepsilon_j|}\right) \tag{33}$$

where F_i denotes the corrected dataset, and X_i denotes the original dataset of budget components. Since ET does not participate in the redistribution of the residual error x based on the example above, the weighting vector is defined as G=[1, 0, −1, −1]. The term Ɛ represents the error in budget components estimated using existing BCC methods, as described in Section 3.2.

Third, the IWE-Res curve is plotted (Fig. 2) to provide an intuitive comparison between the introduced budget component errors and the remaining water imbalance error. The error calculation results from Equations (30) and (31) are presented within the same coordinate system.

The IWE-Res method is illustrated in Fig. 2 using four curves. The x-axis represents the percentage of water imbalance error redistributed to budget components using existing BCC methods, while the y-axis denotes the percentage of the remaining

https://doi.org/10.5194/egusphere-2025-990
Preprint. Discussion started: 22 April 2025

water imbalance error (ΔRes*) after each iteration. The black dashed line represents the redistributed x-error value among the budget components. The thin blue solid line represents the ΔRes* error curve. Since the sum of redistributed x and remaining ΔRes* equals the total ΔRes error, this curve forms a monotonically decreasing 45° line. The thin green solid line represents the introduced budget component error (IWE) after a given percentage of ΔRes is redistributed (x-axis), with its shape varying depending on the redistribution process (Fig. 2 is illustrative). Initially, when no ΔRes is redistributed ($x = 0$), the IWE error is zero. As more ΔRes is redistributed (with increasing x values), IWE increases due to the growing uncertainty introduced. The thin red solid line represents the total error, defined as the sum of ΔRes* and IWE after applying BCC methods. This curve varies depending on the redistribution process, and its minimum value identifies the optimal balance where combined ΔRes* and IWE errors are minimized. The intersection of the ΔRes* and IWE curves indicates only the point at which these errors are equal, not necessarily the optimal balance.

To determine the optimal redistribution of the water imbalance error, we plot the IWE-Res curve (the green solid line) for each basin, identifying the minimum of the red total error curve. We then analyze its patterns across basins with different characteristics to optimize water budget closure and improve the accuracy of budget component datasets.

The IWE error in Fig. 2 also serves as a metric for evaluating the performance of existing BCC methods. If a BCC method perfectly redistributed ΔRes without

https://doi.org/10.5194/egusphere-2025-990
Preprint. Discussion started: 22 April 2025

introducing additional errors, the IWE curve would be a flat line at zero, and the red total error line would coincide with the blue ΔRes* error line. This scenario indicates that full redistribution of water imbalance error achieves the optimal balance, providing indirect validation of the IWE-Res method's effectiveness.

Finally, the optimal balance is identified, enabling the generation of a high-precision dataset that improves water budget closure. The optimal balance corresponds to the minimum of the total error curve (IWE + ΔRes*), where the sum of remaining water imbalance error and introduced budget component errors is minimized. Ideally, both ΔRes* and IWE would reach their minimum values simultaneously, meaning minimal error is introduced while fully redistributing ΔRes. However, since this ideal state may not always be achievable, identifying the point where combined error is minimized is essential. This principle defines the proposed IWE-Res method (Fig. 2).

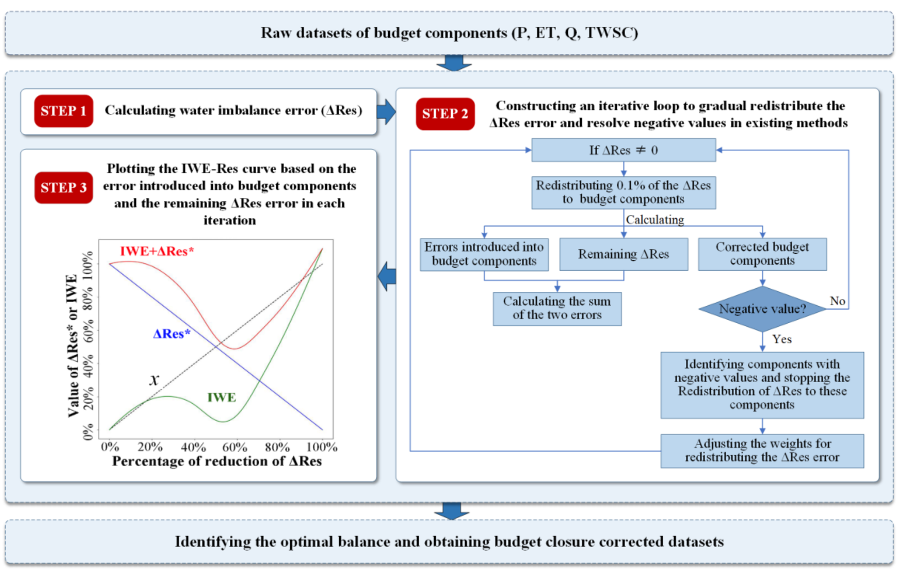

Fig. 2 Framework of the IWE-Res method to identify the optimal balance for

https://doi.org/10.5194/egusphere-2025-990
Preprint. Discussion started: 22 April 2025

redistributing the ΔRes error. The x-axis represents the proportion of ΔRes redistributed to budget components, while the y-axis reflects the proportion of the remaining ΔRes error. The black dashed line represents the redistributed x-error value among the budget components. The blue solid line represents the ΔRes* curve, while the green solid line shows the IWE error introduced into budget components after redistributing the corresponding percentage of ΔRes. The red solid line represents the total error curve.

4 Results

4.1 Water imbalance error

This section presents a comparative analysis of variations in water imbalance errors across different basins and data combinations, aiming to clarify how errors in budget components contribute to these discrepancies. Figure 3 illustrates the spatial distribution of monthly ΔRes errors across various data combinations. To prevent the cancellation of positive and negative values, the absolute values of monthly ΔRes errors were first computed for each basin and then averaged.

As shown in Figure 3, ΔRes values vary significantly across basins. Most basins in Africa, South America, and Europe exhibit high ΔRes values, typically exceeding 20 mm. In North America, ΔRes values generally range from 15 to 45 mm. Due to inconsistencies among budget component datasets, substantial differences in ΔRes also emerge across different data combinations. In combinations where only P data varied while other budget component datasets remained constant (combinations in Fig.

https://doi.org/10.5194/egusphere-2025-990
Preprint. Discussion started: 22 April 2025

3 where the first digit varies while the second and third remain constant), pronounced changes in water imbalance errors were observed in parts of southern Africa, northern Asia, and North America. This suggests substantial estimation errors in P for these regions.

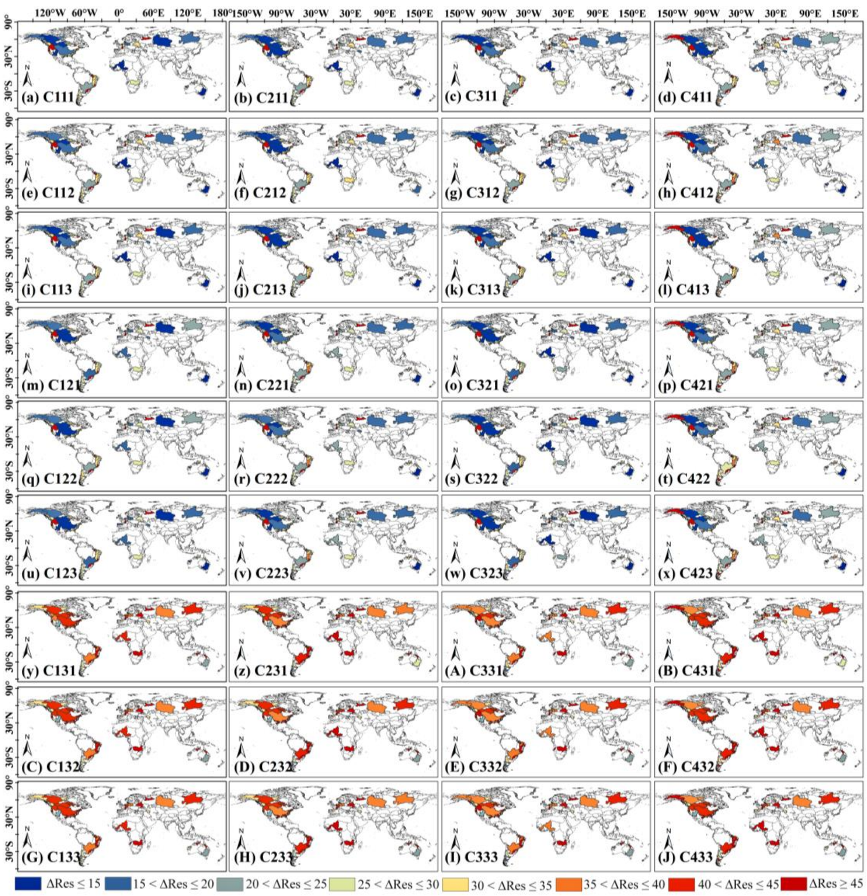

Fig. 3 Spatial distribution of the ΔRes error on a monthly scale for different combinations of budget components. The unit of ΔRes is mm. Each subplot represents a distinct combination, where the first digit corresponds to the P product, the second to the ET product, and the third to the TWSC product. The detailed definitions of

https://doi.org/10.5194/egusphere-2025-990
Preprint. Discussion started: 22 April 2025

these combinations are provided in Equation 3.

When different ET products were used (combinations where the second digit varies while the first and third remain constant), water imbalance errors changed significantly in most basins. Specifically, in combinations using the TerraClimate ET dataset, water imbalance errors exceeded 35 mm in the majority of basins, indicating severe water imbalance. This underscores the considerable discrepancies among ET products and their substantial impact on accurately representing basin water balance. In contrast, when TWSC data from different GRACE products were used (combinations where the third digit varies while the first and second remain constant), variations in water imbalance errors across basins were relatively small.

Overall, ET and P are the primary variables influencing water imbalance in most basins, consistent with previous findings (Pan et al., 2012; Zhang et al., 2018). The uncertainty in budget component datasets remains a key challenge for water balance research (Dagan et al., 2019; Lv et al., 2017; Luo et al., 2023).

4.2 Uncertainties of budget components introduced by closing water budget

To gain a more comprehensive understanding of the uncertainties introduced into budget components when closing the water budget, this section analyzes the errors introduced by fully closing the water budget using existing BCC methods from three perspectives: the errors of individual budget components, the occurrence of negative values, and ensemble errors (Section 3.3).

4.2.1 Errors of individual budget components

https://doi.org/10.5194/egusphere-2025-990
Preprint. Discussion started: 22 April 2025

Figure 4 presents the relative statistical metrics calculated using Equations 19–22 to evaluate the uncertainties introduced into budget components by existing BCC methods. Positive values indicate an improvement in the accuracy of corrected budget components, whereas negative values indicate a decline in accuracy.

Overall, existing BCC methods exhibit notable limitations in enhancing the accuracy of budget components. In particular, for P, nearly all statistical metrics (CC', NSE', MAE', RMSE') across various basins yield negative values. For instance, under the CKF method, these values are approximately –0.05, –0.15, –3.82 mm, and –8.47 mm, respectively, indicating a significant reduction in the accuracy of the corrected P dataset when BCC methods are applied to enforce water budget closure. Specifically, the accuracy of the corrected P dataset decreases by approximately 6%, 34%, 11%, and 55%, as reflected in the CC, NSE, MAE, and RMSE metrics, respectively. Analysis of 13 selected basins with sufficient P observations further confirms this decline, showing a reduction in the accuracy of budget-corrected P (Figure 5). A possible explanation for this decrease is the inherently high accuracy of raw P datasets, supported by advancements in remote sensing technologies, meteorological models, and observational networks. However, when BCC methods are applied, water imbalance errors from other budget components, such as ET, may be inappropriately redistributed to the corrected P dataset in an effort to enforce overall water budget closure. As a result, while the total water budget is balanced, the accuracy of the corrected P data is compromised.

https://doi.org/10.5194/egusphere-2025-990
Preprint. Discussion started: 22 April 2025

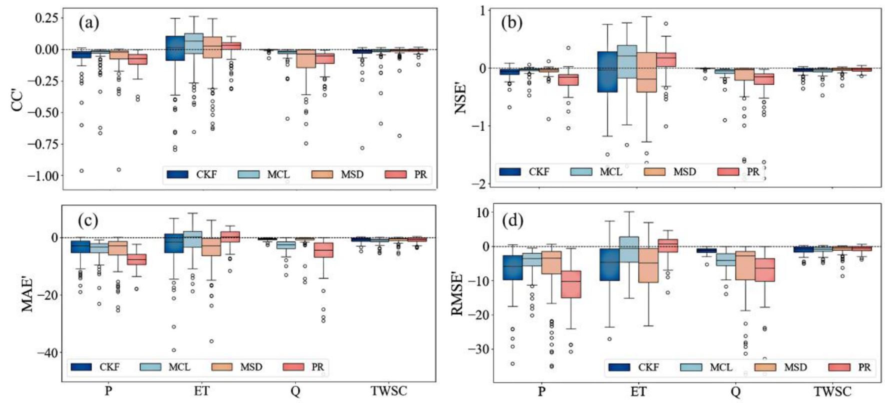

Fig. 4 Box plot quantifying the errors introduced into budget components by existing BCC methods when closing the water budget. (a) - (d) represent the results of the CC', NSE', MAE', RMSE' indicators, respectively. Positive values indicate an improvement in accuracy relative to the reference values after applying existing BCC methods, while negative values indicate a decline. Different colors represent different BCC methods.

The impact of enforcing water budget closure using existing BCC methods on ET was particularly significant (Fig. 4), with approximately 50% of basins exhibiting improved accuracy in corrected ET. For TWSC, most basins showed decreased accuracy. For Q, CC' and NSE' values ranged from 0 to -0.5, while MAE' and RMSE' were primarily concentrated between 0 mm and -20 mm. Consequently, the accuracy of corrected Q declined, with CC, NSE, MAE, and RMSE decreasing by approximately 0.1, 0.2, 3 mm, and 5 mm, respectively. These findings indicate that while redistributing the entire ΔRes enhances the consistency of budget components, it provides limited improvement in their accuracy and may even introduce further

https://doi.org/10.5194/egusphere-2025-990
Preprint. Discussion started: 22 April 2025

errors. Identifying an optimal redistribution strategy for ΔRes errors could help mitigate this issue.

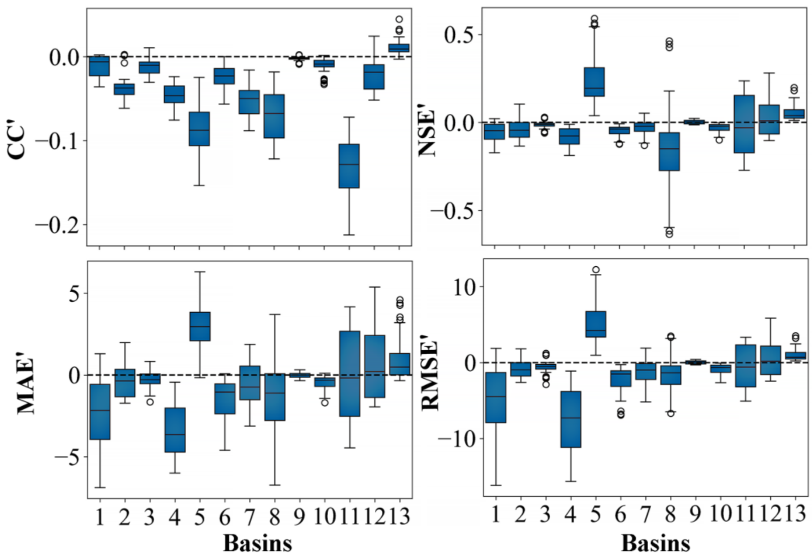

Fig. 5 Box plot illustrating precipitation errors introduced by correcting ΔRes using existing BCC methods across 13 basins with sufficient observational precipitation data. The x-axis represents the 13 basins in the following order: NIGER, OB, MISSISSIPPI, SACRAMENTO, SAN JOAQUIN, SUSQUEHANNA, BRAZOS, FRASER, NELSON, MURRAY, RIO EBRO, ELBE, and KURA.

4.2.2 Negative values

This section examines the occurrence of negative values in budget components arising from the application of existing BCC methods to close the water budget. For each budget component, the proportion of months with negative values relative to the total time series was computed (Fig. 6). Overall, the fraction of negative values across budget components ranges from 0% to 10%, with the majority falling below 5%. This

https://doi.org/10.5194/egusphere-2025-990
Preprint. Discussion started: 22 April 2025

proportion is notable, as negative values indicate substantial inaccuracies in the redistribution of water imbalance errors by existing BCC methods. When a budget component exhibits a negative value, the accuracy of the remaining budget components is also compromised. The relatively high occurrence of negative values highlights the need for methodological improvements to enhance the performance of existing BCC methods.

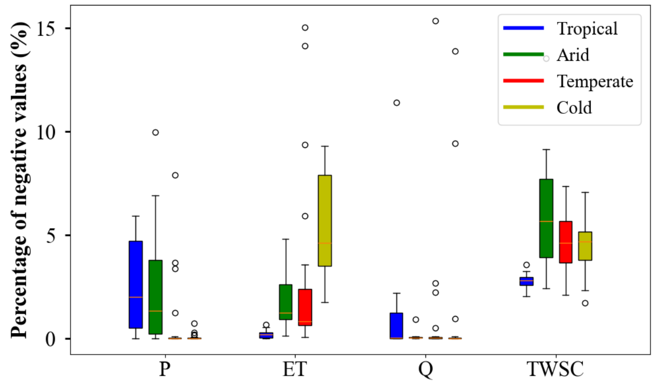

Fig. 6 Percentage of negative values for corrected datasets of budget components induced by closing the water budget. Different colors indicate distinct climate classifications.

Among the individual budget components, ET and TWSC exhibit the most pronounced negative values, followed by P, while Q shows the least (Fig. 6). Notably, the proportion of negative values in budget components varies significantly across climate types. For P, negative values generally remain below 5% but can occasionally reach 7% in arid regions. The likelihood of negative P values is higher in tropical and arid climates (mostly below 5%) compared with temperate and cold regions (around

https://doi.org/10.5194/egusphere-2025-990
Preprint. Discussion started: 22 April 2025

1%). For ET, the proportion of negative values is largely below 5%, but it is notably higher in cold climates (reaching 9%), followed by arid and temperate regions (approximately 1%–3%). Tropical climates exhibit the lowest proportion of negative ET values, with most instances below 1%. Q consistently shows a low occurrence of negative values across all climate types (generally below 3%), with a slightly higher probability in tropical regions than in other zones. The proportion of negative TWSC values ranges from 3% to 10%, being lowest in tropical climates (below 5%), while other climate types exhibit values between 3% and 10%.

Fig. 7 presents the seasonal cycle of negative values across different climate zones, examining whether these values exhibit significant seasonal patterns. Negative P values predominantly occur in summer and autumn, with a higher proportion from June to September in tropical climates compared to arid regions. ET tends to show negative values more frequently in winter and spring, with a lower likelihood in summer and autumn. Except in summer, cold climate zones are most susceptible to negative ET values. Among the four budget components, Q has the lowest occurrence of negative values. Negative TWSC values are primarily observed in spring, autumn, and December, with arid regions exhibiting a higher likelihood of negative values throughout the year compared to other climate types. These findings indicate that the occurrence of negative values varies significantly across seasons and climate zones. Future research should account for this seasonal variability to further refine existing BCC methods.

https://doi.org/10.5194/egusphere-2025-990
Preprint. Discussion started: 22 April 2025

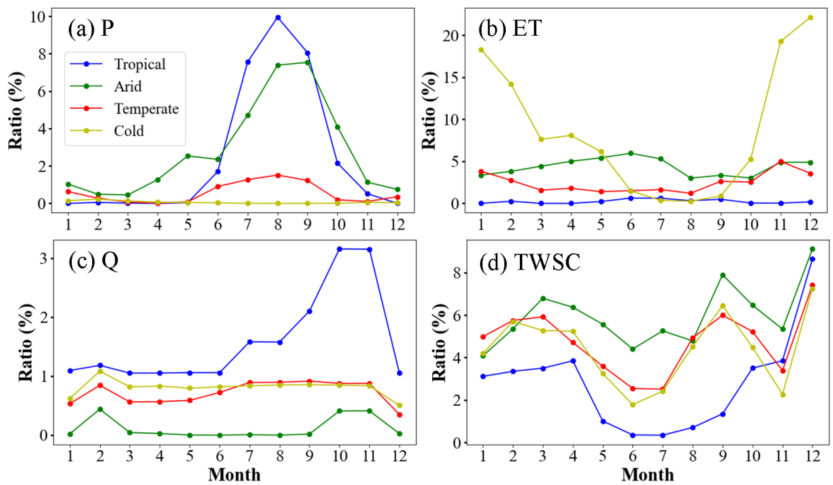

Fig. 7 Seasonal cycle of the proportion of negative errors for budget components. Different colors representing various climate types.

4.2.3 Ensemble errors

Fig. 8 presents the ensemble errors in budget components (i.e., F(Re) in Equation 27) introduced by existing BCC methods (CKF, MCL, MSD, and PR). All four methods exhibit similar spatial distribution patterns. Notably, high ensemble errors (F(Re) > 10%) are concentrated in the northwestern basins of North America, particularly in Alaska, suggesting substantial variations in budget components in these regions. Basins with minor ensemble errors (5% < F(Re) ≤ 10%) generally cover larger areas, such as African and Northern Asia. Although these errors are relatively small, they remain non-negligible. Basins with lower ensemble errors (F(Re) ≤ 5%) also cover some basins. Further analysis of ΔRes in basins with higher F(Re) values reveals a strong correlation, as these basins also exhibit larger ΔRes. This finding highlights the limitations of existing BCC methods in effectively redistributing ΔRes

https://doi.org/10.5194/egusphere-2025-990
Preprint. Discussion started: 22 April 2025

errors.

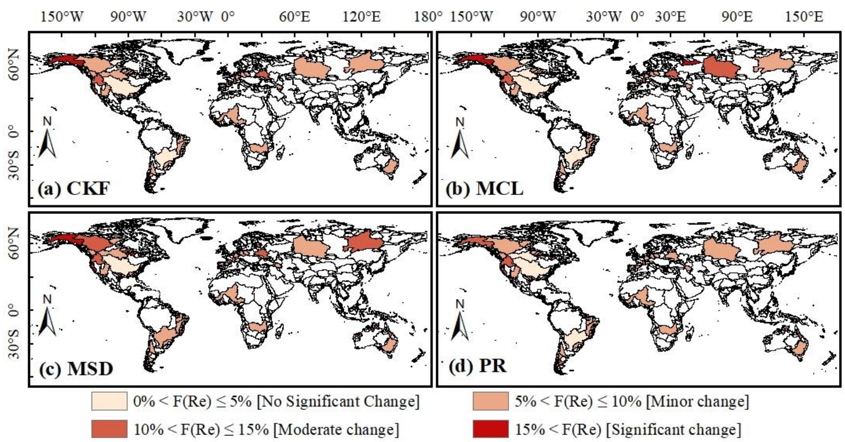

Fig. 8 Ensemble errors in budget components introduced by closing the water budget using existing BCC methods.

To determine whether the error cost introduced by existing BCC methods in closing the water budget outweighs the reduction in water imbalance error, we analyzed the relationship between the reduction in ΔRes error and the introduced budget component errors (Fig. 9). As shown in Fig. 9, with the exception of the PR method, the basins where |RAE| exceeds |Res| are largely consistent across the other three BCC methods. This discrepancy arises because the PR method redistributes ΔRes based on the magnitude of budget components, whereas the CKF, MCL, and MSD methods redistribute ΔRes according to the estimated errors in budget components.

https://doi.org/10.5194/egusphere-2025-990
Preprint. Discussion started: 22 April 2025

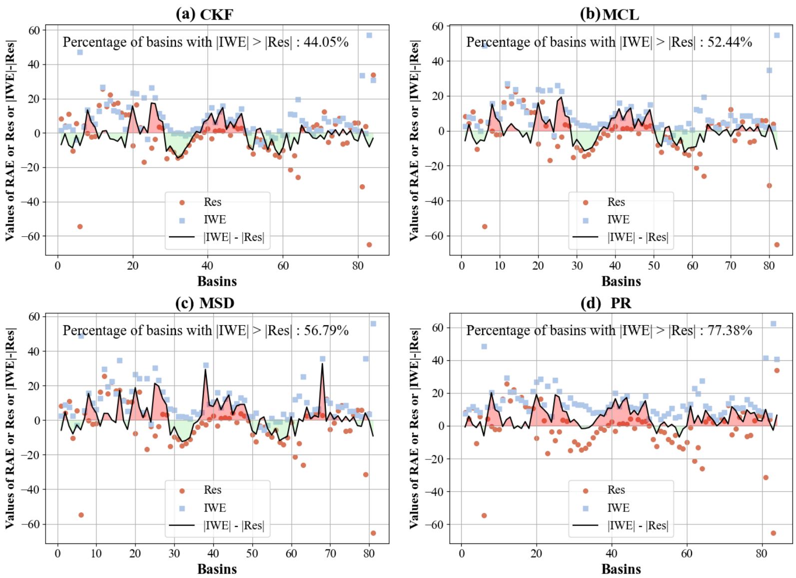

Fig. 9 Comparison of relative absolute error (RAE) and residual error (Res) for four BCC methods (CKF, MCL, MSD, PR) across various basins. The black lines in the red shaded area on the upper half of the y-axis indicate that the error introduced by the BCC methods for budget components exceeds the reduction in ΔRes error (|RAE| > |Res|), while the green shaded area on the lower half of the y-axis represents cases where the error introduced is less than the reduction in ΔRes error (|RAE| < |Res|).

For the CKF, MCL, MSD, and PR methods, the proportions of basins where |RAE| exceeds |Res| are 44.05%, 52.44%, 56.79%, and 77.38%, respectively. This indicates that, for all four methods, the introduced |RAE| error in budget components surpasses the reduction in water imbalance error in more than 40% of the basins. These findings underscore the non-negligible uncertainties introduced by these methods. Striking a balance between reducing water imbalance error and minimizing

https://doi.org/10.5194/egusphere-2025-990
Preprint. Discussion started: 22 April 2025

the impact of budget component errors remains a critical challenge, motivating us to propose the IWE-Res method to identify optimal balance.

4.3 Verifying the accuracy of the proposed IWE-Res method

Based on the error analysis of existing BCC methods in Section 4.2, this section assesses the accuracy and reliability of the proposed IWE-Res method. The evaluation is conducted through a comparative analysis with PR, CKF, MCL, and MSD, focusing on three key aspects: the errors of individual budget components, the occurrence of negative values, and ensemble errors.

Fig. 10 compares the accuracy of the proposed IWE-Res method with existing PR, CKF, MCL, and MSD methods from the perspective of errors in individual budget components. The red and blue lines represent the IWE-Res method and the existing BCC methods, respectively, while the bars indicate the relative accuracy improvement of the IWE-Res method compared to the BCC methods. As shown in Fig. 10, the proposed IWE-Res method exhibits consistently higher accuracy than all existing CKF, MCL, MSD, and PR methods for budget components P, ET, Q, and TWSC. This result highlights the superior capability of the IWE-Res method in optimizing errors in budget corrected datasets. According to the statistical metrics CC, NSE, MAE, and RMSE, the proposed IWE-Res method improves the corrected P data by 4.2%, 21.3%, 25.5% and 29.5%, respectively, compared to the existing BCC methods. For corrected ET, the improvements are 6.9%, 265.7%, 17.6% and 24.7%, respectively; for corrected Q, the improvements are 3.4%, 185.1%, 67.1%, and 69.0%; and for corrected TWSC, the improvements are 0.0%, 7.0%, 7.5%, and 6.8%.

https://doi.org/10.5194/egusphere-2025-990
Preprint. Discussion started: 22 April 2025

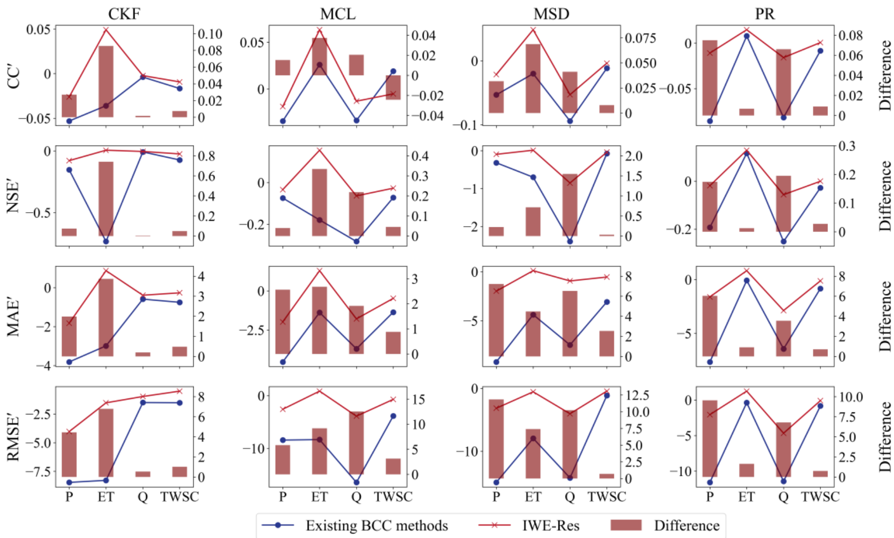

Fig. 10 Performance comparison of the proposed IWE-Res method with existing BCC methods in corrected individual budget components. The red and blue lines in the figure represent the average values across all basins considered in this study.

Table 2 presents the percentage of negative values observed in the corrected budget components for the proposed IWE-Res method and existing BCC methods. One of the key contributions of the IWE-Res method is its ability to address the critical limitation of negative value generation in existing BCC methods. As a result, the percentage of negative values in the corrected P, ET, Q, and TWSC data using the proposed IWE-Res method is zero. In contrast, the corrected P, ET, Q, and TWSC data obtained from existing BCC methods contain negative values to varying degrees (for a detailed analysis of negative values, see Section 4.2.2). These results demonstrate that, in addition to improving the accuracy of budget components relative to observations, the proposed IWE-Res method effectively eliminates the issue of

https://doi.org/10.5194/egusphere-2025-990
Preprint. Discussion started: 22 April 2025

negative values inherent in existing BCC methods.

Table 2 The percentage of months with negative values in the corrected datasets of budget components P, ET, Q, and TWSC for the proposed IWE-Res method and existing BCC methods. The percentages in the table represent the average values across all basins considered in this study.

	P		**ET**		**Q**		**TWSC**	
	Existing	IWE-Res	Existing	IWE-Res	Existing	IWE-Res	Existing	IWE-Res
CKF	0.31%	0%	6.73%	0%	0.75%	0%	4.81%	0%
MCL	1.82%	0%	4.78%	0%	0.77%	0%	7.61%	0%
MSD	1.68%	0%	7.03%	0%	0.82%	0%	5.40%	0%
PR	0%	0%	0.57%	0%	0.72%	0%	0.47%	0%

We further evaluate the accuracy and reliability of the proposed IWE-Res method using the ensemble error metric defined by Equation (27) (Fig. 11), where lower values indicate better model performance. As shown in Fig. 11, the IWE-Res method significantly reduces ensemble errors compared to existing BCC methods. For instance, in the CKF method, the median ensemble error decreases from above 5% to below 5%. This reduction is even more pronounced in the MCL, MSD, and PR methods. Additionally, the interquartile ranges under IWE-Res are notably narrower, suggesting improved control over stochastic variability. For example, in the PR method, the interquartile range shrinks from 5–8% (existing BCC methods) to 1–2% (IWE-Res), reflecting an approximate 67% reduction in variability. These findings highlight the robustness of the IWE-Res method in minimizing integrated errors, aligning with its previously demonstrated excellence in single-variable error optimization and negative value elimination.

https://doi.org/10.5194/egusphere-2025-990
Preprint. Discussion started: 22 April 2025

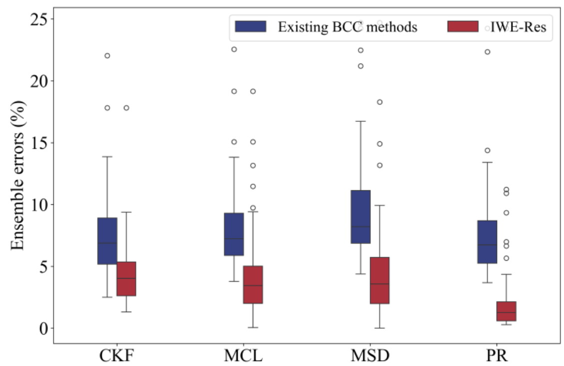

Fig. 11 Performance comparison of the proposed IWE-Res method and existing BCC methods based on the ensemble errors of budget components.

4.4 Identifying the optimal balance for redistributing water imbalance error

Based on the proposed IWE-Res method, this section aims to determine the optimal balance for redistributing water imbalance errors across different climate zones (Tropical, Arid, Temperate, and Cold climate zones) to achieve the best trade-off (Figs. 12-15). Specifically, it seeks to minimize both water imbalance errors and the uncertainties in budget components introduced by enforcing water budget closure. The findings offer a valuable reference for generating high-precision datasets of budget components with a closed water budget in diverse climate regions. When developing the IWE-Res method, we incorporated multiple BCC methods, each based on different principles. As a result, the identified optimal balance results vary across methods. This section presents results for the CKF method only, while results for the MSD, MCL, and PR methods are provided in the supplementary materials.

Overall, the optimal balance varied among basins located in different climate zones (Figs. 12–15). In most basins within the Tropical, Arid, and Temperate zones,

https://doi.org/10.5194/egusphere-2025-990
Preprint. Discussion started: 22 April 2025

the optimal balance was achieved when only a portion of the water imbalance error, rather than the entire error, was redistributed to budget components. However, this pattern was not observed in the Cold region.

For most basins in the Tropical climate zone (Fig. 12), the optimal balance was reached when 40%–90% of ΔRes was reallocated to budget components, suggesting that the corrected budget datasets achieve their highest accuracy within this range. Notably, approximately 20% of basins attained their optimal balance when 80%–90% of ΔRes was redistributed, while about 70% did so within the 40%–50% range. Therefore, in Tropical basins, if sufficient observational data are unavailable to precisely determine the optimal balance, redistributing 40%–50% of ΔRes to budget components is recommended to obtain the most accurate dataset.

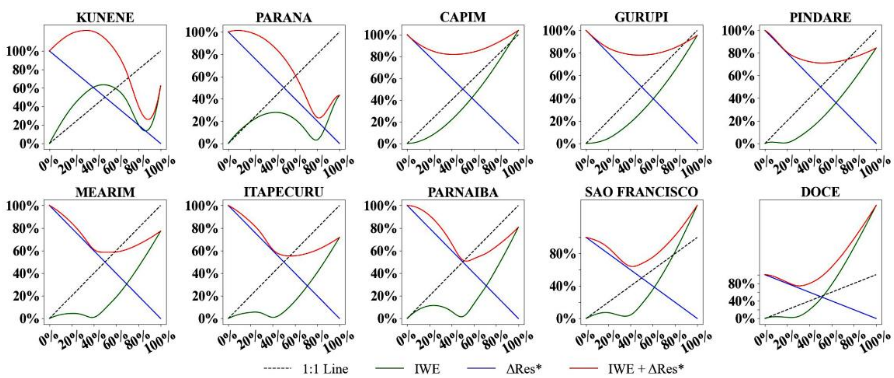

Fig. 12 IWE-Res curve in basins of Tropical climate zone for identifying the optimal balance that enhances water budget closure and reduces uncertainty.

For basins in the Arid climate zone (Fig. 13), optimal balance are generally found when 40%–90% of ΔRes is redistributed, indicating that the corrected budget

https://doi.org/10.5194/egusphere-2025-990
Preprint. Discussion started: 22 April 2025

component datasets achieve their highest accuracy within this range. Specifically, approximately 31% of basins reach their optimal balance at 40%–50% redistribution, 38% at 60%–80%, and over 20% at 90%. Thus, the distribution of optimal balance in Arid basins does not follow a distinct pattern.

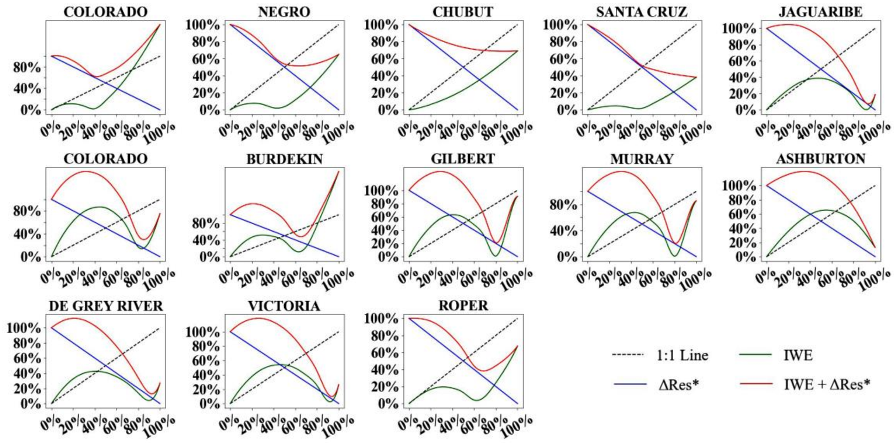

Fig. 13 IWE-Res curve in watersheds of Arid climate zone for identifying the optimal balance that enhances water budget closure and reduces uncertainty.

In the Temperate climate zone (Fig. 14), optimal balance are concentrated within the 40%–90% range. Approximately 53% of basins achieve their optimal balance when 40%–50% of ΔRes is redistributed, while 17% and 13% reach it at 70% and 90% of the ΔRes redistribution. A smaller proportion of basins achieve optimal balance at 60% and 80% of the ΔRes redistribution. Overall, redistributing 40%–50% of ΔRes minimizes the combined error from both the introduced budget component error and the remaining water imbalance error in most basins.

https://doi.org/10.5194/egusphere-2025-990
Preprint. Discussion started: 22 April 2025

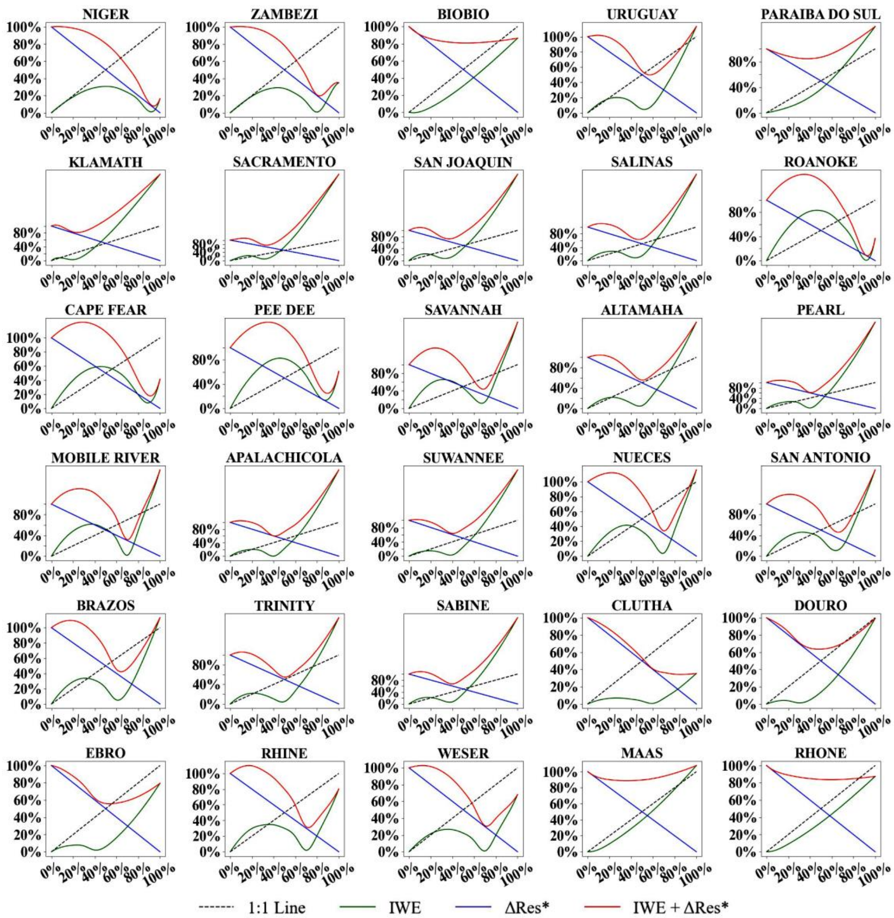

Fig. 14 IWE-Res curve in watersheds of Temperate climate zone for identifying the optimal balance that enhances water budget closure and reduces uncertainty.

In Cold climate zone basins (Fig. 15), the optimal balance is typically reached when the entire ΔRes is fully redistributed. This suggests that complete redistribution of ΔRes does not compromise the accuracy of the budget components. This is primarily due to the trend observed in the IWE curve, which initially increases—indicating rising error—before decreasing, in contrast to the patterns seen

https://doi.org/10.5194/egusphere-2025-990
Preprint. Discussion started: 22 April 2025

in most basins in Figs. 12–14. A comparison of ΔRes and the negative values introduced by full redistribution of ΔRes across climate zones reveals that, in Cold regions, negative values predominantly occur in ET. This is likely due to the inherently lower ET values in Cold regions, which increases the likelihood of negative values when ΔRes is redistributed. However, errors introduced in other budget components, such as P and Q, remain relatively low under full redistribution of ΔRes.

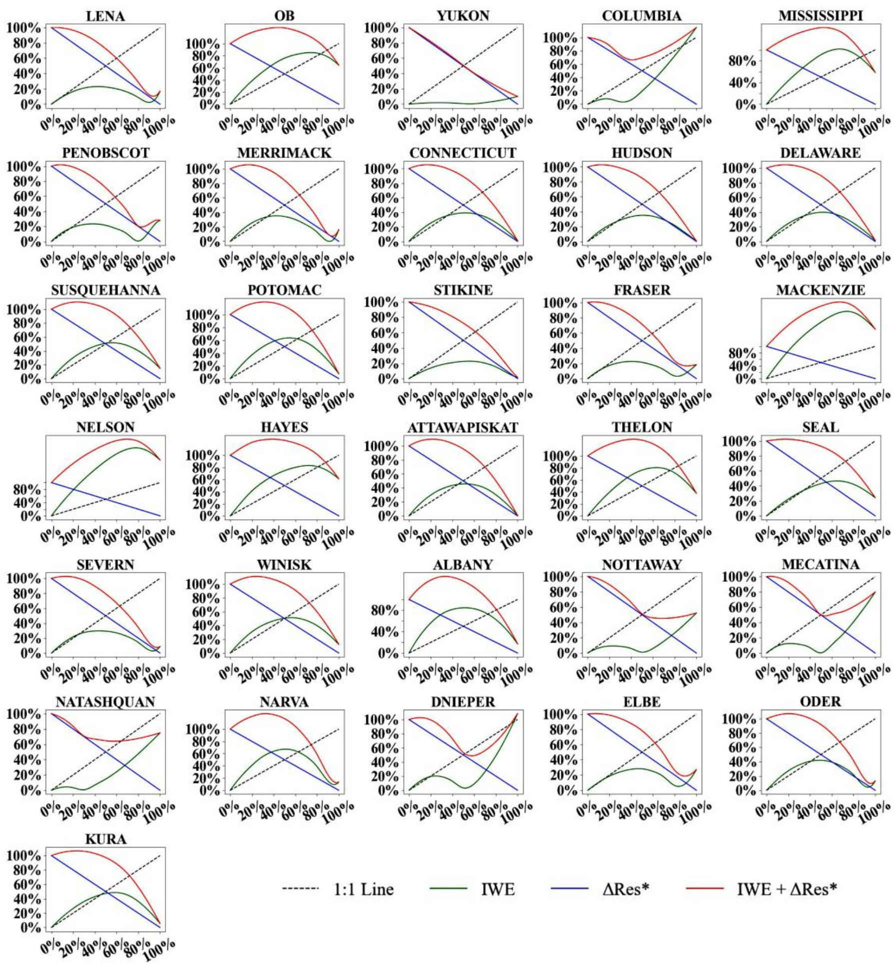

Fig. 15 IWE-Res curve in watersheds of Cold climate zone for identifying the optimal balance that enhances water budget closure and reduces uncertainty.

https://doi.org/10.5194/egusphere-2025-990
Preprint. Discussion started: 22 April 2025

5 Discussion

5.1 Uncertainty introduced by existing BCC methods

To quantify the uncertainty introduced by existing BCC methods in closing the water balance, we evaluated four BCC methods across 84 global basins. The assessment focused on errors in individual budget components, occurrences of negative values, and ensemble errors in budget components. Our findings indicate that while existing BCC methods improve the consistency of budget components, their ability to enhance their accuracy is limited and, in some cases, may even reduce it.

Several factors may contribute to this reduction in accuracy. First, existing BCC methods do not incorporate observational data for budget components; instead, they redistribute water imbalance errors based on estimated errors in each budget component. If these error estimates are inaccurate, additional uncertainty may be introduced. Therefore, incorporating more observational data on budget components represents a key strategy for mitigating this issue. Second, existing BCC methods, including the proposed IWE-Res method, do not account for the physical mechanisms of the water cycle, relying instead on statistical approaches to enforce water budget closure. As a result, the corrected budget components may deviate from actual conditions. Future research should integrate BCC methods with physically based hydrological models to improve the physical consistency of budget component datasets. Third, observational datasets themselves do not fully satisfy water budget closure. Consequently, even if a corrected dataset achieves complete closure using existing methods, this does not necessarily mean it aligns more closely with

https://doi.org/10.5194/egusphere-2025-990
Preprint. Discussion started: 22 April 2025

observational data. In practice, corrected datasets may approach the true values, but without direct access to these true values, evaluating their accuracy remains challenging. Developing more objective methods for assessing the accuracy of water budget closure-corrected datasets will be an important focus for future studies, although this lies beyond the scope of the present study.

5.2 Identification of the optimal balance

Each budget component inherently contains observational or model-based errors. Indiscriminately redistributing water imbalance errors across all budget components to achieve complete water budget closure can introduce additional uncertainties. By identifying the optimal balance for error redistribution across different climate zones, we observed significant variations in distribution patterns. In tropical and temperate regions, most basins achieved their optimal balance when 40%–90% of the water imbalance error was redistributed, with a concentration around the 40%–50% range. In arid regions, the distribution of optimal balance was more dispersed, lacking a clear concentration within any specific redistribution range but generally falling within the 40%–90% range. Cold climate regions exhibited distinct characteristics, with most basins achieving the smallest error when the water imbalance error was fully redistributed.

Overall, determining an appropriate redistribution ratio for water imbalance errors effectively improves budget component accuracy. Future research should focus on the underlying rationale for error redistribution, as the sensitivity of different budget components to water imbalance errors varies. Excessive or insufficient

https://doi.org/10.5194/egusphere-2025-990
Preprint. Discussion started: 22 April 2025

redistribution to certain components can lead to imbalances in the remaining components, ultimately failing to accurately represent actual hydrological processes.

6 Conclusions

Existing BCC methods introduce new uncertainties when closing the water budget due to challenges in accurately estimating errors in budget components and the integrated concept of water imbalance error. This study first evaluates the issues arising from existing BCC methods by comparing the errors introduced in budget components with the improvement in water budget closure precision. A new method, termed IWE-Res, is proposed to identify the optimal redistribution of ΔRes, aiming to minimize the sum of the remaining residual error and the introduced budget component error. To assess the reliability of the IWE-Res method, we compare it with four different BCC methods across 84 basins spanning various global climate zones. The main conclusions are as follows:

(1) While applying existing BCC methods reduces water imbalance error, it simultaneously introduces new errors in budget components. For P, a decline in accuracy is observed in most basins. For Q, the corrected data exhibits lower performance than the raw data, with reductions in CC, NSE, MAE, and RMSE of approximately 0.1, 0.2, 3 mm, and 5 mm, respectively. At the basin scale, more than 40% of basins experience budget component errors greater than the reduction in ΔRes after applying existing BCC methods.

(2) The proportion of negative corrected values in each budget component is predominantly within 0%–5%. For ET, negative corrected values are mostly below

5%, though they reach 9% in cold climate regions. For P, the proportion is primarily below 5%, with rare occurrences around 7%. Q generally exhibits a lower proportion of negative values, mostly below 3%. In TWSC, negative values are concentrated between 3% and 10%.

(3) The proposed IWE-Res method improves the accuracy of corrected budget components compared to existing BCC methods. Based on RMSE, it improves the accuracy of corrected P by 29.5%, corrected ET by 24.7%, corrected Q by 69.0%, and corrected TWSC by 6.8%.

(4) Except in cold regions, redistributing 40%–90% of ΔRes to budget components yields the optimal balance, minimizing the sum of the remaining ΔRes and the introduced budget component error. In tropical and temperate regions, the optimal balance is typically achieved when 40%–50% of ΔRes is redistributed. Similarly, in arid regions, redistributing 40%–90% of ΔRes effectively reduces errors, though the optimal redistribution ratio varies across basins. In most cold-region basins, the total error is minimized when the entire ΔRes is redistributed.

Declaration of Competing Interest

The authors declare that they have no known competing financial interests or personal relationships that could have appeared to influence the work reported in this paper.

Acknowledgments

This research was supported by the National Natural Science Foundation of China (No. 42201038) and China Scholarship Council.

https://doi.org/10.5194/egusphere-2025-990
Preprint. Discussion started: 22 April 2025

Reference

Abatzoglou, J. T., Dobrowski, S. Z., Parks, S. A., & Hegewisch, K. C. (2018). TerraClimate, a high-resolution global dataset of monthly climate and climatic water balance from 1958–2015. *Scientific Data, 5*(1), 1-12. https://doi.org/10.1038/sdata.2017.191

Abhishek, Kinouchi, T., Abolafia-Rosenzweig, R., & Ito, M. (2021). Water budget closure in the Upper Chao Phraya River basin, Thailand using multisource data. *Remote Sensing, 14*(1), 173. https://doi.org/10.3390/rs14010173

Abolafia-Rosenzweig, R., Pan, M., Zeng, J., & Livneh, B. (2021). Remotely sensed ensembles of the terrestrial water budget over major global river basins: An assessment of three closure techniques. *Remote Sensing of Environment, 252*, 112191. https://doi.org/10.1016/j.rse.2020.112191

Aires, F. (2014). Combining datasets of satellite-retrieved products. Part I: Methodology and water budget closure. *Journal of Hydrometeorology, 15*(4), 1677-1691. https://doi.org/10.1175/JHM-D-13-0148.1

Beck, H. E., Pan, M., Roy, T., Weedon, G. P., Pappenberger, F., Van Dijk, A. I., . . . Wood, E. F. (2019). Daily evaluation of 26 precipitation datasets using Stage-IV gauge-radar data for the CONUS. *Hydrology and Earth System Sciences, 23*(1), 207-224. https://doi.org/10.5194/hess-23-207-2019

Beck, H. E., Vergopolan, N., Pan, M., Levizzani, V., Van Dijk, A. I., Weedon, G. P., . . . Wood, E. F. (2017). Global-scale evaluation of 22 precipitation datasets using gauge observations and hydrological modeling. *Hydrology and Earth System*

https://doi.org/10.5194/egusphere-2025-990
Preprint. Discussion started: 22 April 2025

Sciences, 21(12), 6201-6217. https://doi.org/10.5194/hess-21-6201-2017

Beck, H. E., Wood, E. F., Pan, M., Fisher, C. K., Miralles, D. G., Van Dijk, A. I., . . . Adler, R. F. (2019). MSWEP V2 global 3-hourly 0.1 precipitation: methodology and quantitative assessment. *Bulletin of the American Meteorological society, 100*(3), 473-500. https://doi.org/10.1175/BAMS-D-17-0138.1

Becker, A., Finger, P., Meyer-Christoffer, A., Rudolf, B., Schamm, K., Schneider, U., & Ziese, M. (2013). A description of the global land-surface precipitation data products of the Global Precipitation Climatology Centre with sample applications including centennial (trend) analysis from 1901–present. *Earth System Science Data, 5*(1), 71-99. https://doi.org/10.5194/essd-5-71-2013

Burek, P., & Smilovic, M. (2022). The use of GRDC gauging stations for calibrating large-scale hydrological models. *Earth System Science Data Discussions, 2022*, 1-18. https://doi.org/10.5194/essd-15-5617-2023

Boergens, E., Güntner, A., Sips, M., Schwatke, C., & Dobslaw, H. (2024). Interannual variations of terrestrial water storage in the East African Rift region. *Hydrology and Earth System Sciences, 28*(20), 4733-4754. https://doi.org/10.5194/hess-28-4733-2024Chen, X., Su, Z., Ma, Y., Trigo, I., & Gentine, P. (2021). Remote sensing of global daily evapotranspiration based on a surface energy balance method and reanalysis data. *Journal of Geophysical Research: Atmospheres, 126*(16), e2020JD032873. https://doi.org/10.1029/2020JD032873

https://doi.org/10.5194/egusphere-2025-990
Preprint. Discussion started: 22 April 2025

Crosbie, R., Pollock, D., Mpelasoka, F., Barron, O., Charles, S., & Donn, M. (2012). Changes in Köppen-Geiger climate types under a future climate for Australia: hydrological implications. *Hydrology and Earth System Sciences, 16*(9), 3341-3349. https://doi.org/10.5194/hess-16-3341-2012

Dagan, G., Stier, P., & Watson-Parris, D. (2019). Analysis of the atmospheric water budget for elucidating the spatial scale of precipitation changes under climate change. *Geophysical Research Letters, 46*(17-18), 10504-10511.

Dastjerdi, P. A., Ghomlaghi, A., & Nasseri, M. (2024). A new approach to ensemble precipitation Estimation: Coupling satellite hydrological products with backward water balance models in Large-Scale. *Journal of Hydrology, 629*, 130564. https://doi.org/10.1016/j.jhydrol.2023.130564

Famiglietti, J. S., Lo, M., Ho, S. L., Bethune, J., Anderson, K., Syed, T. H., . . . Rodell, M. (2011). Satellites measure recent rates of groundwater depletion in California's Central Valley. *Geophysical Research Letters, 38*(3). https://doi.org/10.1029/2010GL046442

Hansford, M. R., Plink-Björklund, P., & Jones, E. R. (2020). Global quantitative analyses of river discharge variability and hydrograph shape with respect to climate types. *Earth-science reviews, 200*, 102977. https://doi.org/10.1016/j.earscirev.2019.102977

Hsu, K.-l., Gao, X., Sorooshian, S., & Gupta, H. V. (1997). Precipitation estimation from remotely sensed information using artificial neural networks. *Journal of Applied Meteorology and Climatology, 36*(9), 1176-1190.

https://doi.org/10.5194/egusphere-2025-990
Preprint. Discussion started: 22 April 2025

https://doi.org/10.1175/1520-0450(1997)036<1176:PEFRSI>2.0.CO;2

Huffman, G. J., Bolvin, D. T., Braithwaite, D., Hsu, K., Joyce, R., Xie, P., & Yoo, S.-H. (2015). NASA global precipitation measurement (GPM) integrated multi-satellite retrievals for GPM (IMERG). *Algorithm theoretical basis document (ATBD) version, 4*(26), 2020-2005.

Jiménez, C., Martens, B., Miralles, D. M., Fisher, J. B., Beck, H. E., & Fernández-Prieto, D. (2018). Exploring the merging of the global land evaporation WACMOS-ET products based on local tower measurements. *Hydrology and Earth System Sciences, 22*(8), 4513-4533. https://doi.org/10.5194/HESS-22-4513-2018

Landerer, F. W., Flechtner, F. M., Save, H., Webb, F. H., Bandikova, T., Bertiger, W. I., . . . Dobslaw, H. (2020). Extending the global mass change data record: GRACE Follow-On instrument and science data performance. *Geophysical Research Letters, 47*(12), e2020GL088306. https://doi.org/10.1029/2020GL088306

Lehmann, F., Vishwakarma, B. D., & Bamber, J. (2022). How well are we able to close the water budget at the global scale?. Hydrology and Earth System Sciences, 26(1), 35-54. https://doi.org/10.5194/hess-26-35-2022

Li, L., Dai, Y., Wei, Z., Wei, S., Zhang, Y., Wei, N., & Li, Q. (2024). Enforcing Water Balance in Multitask Deep Learning Models for Hydrological Forecasting. *Journal of Hydrometeorology, 25*(1), 89-103. https://doi.org/10.1175/JHM-D-23-0073.1

Liu, X., Yang, K., Ferreira, V. G., & Bai, P. (2022). Hydrologic model calibration with remote sensing data products in global large basins. *Water Resources Research, 58*(12), e2022WR032929. https://doi.org/10.1029/2022WR032929

Luo, Z., Gao, Z., Wang, L., Wang, S., & Wang, L. (2023). A method for balancing the terrestrial water budget and improving the estimation of individual budget components. *Agricultural and Forest Meteorology, 341*, 109667. https://doi.org/10.1016/j.agrformet.2023.109667

Luo, Z., Li, H., Zhang, S., Wang, L., Wang, S., & Wang, L. (2023). A novel two-step method for enforcing water budget closure and an intercomparison of budget closure correction methods based on satellite hydrological products. *Water Resources Research, 59*(3), e2022WR032176. https://doi.org/10.1029/2022WR032176

Luo, Z., Yu, H., Liu, H., & Chen, J. (2023). Assessing the Water Budget Closure Accuracy of Satellite/Reanalysis-Based Hydrological Data Products over Mainland China. *Remote Sensing, 15*(21), 5230.

Lv, M., Ma, Z., Yuan, X., Lv, M., Li, M., & Zheng, Z. (2017). Water budget closure based on GRACE measurements and reconstructed evapotranspiration using GLDAS and water use data for two large densely-populated mid-latitude basins. *Journal of Hydrology, 547*, 585-599.

Miralles, D. G., Holmes, T., De Jeu, R., Gash, J., Meesters, A., & Dolman, A. (2011). Global land-surface evaporation estimated from satellite-based observations. *Hydrology and Earth System Sciences, 15*(2), 453-469.

https://doi.org/10.5194/egusphere-2025-990
Preprint. Discussion started: 22 April 2025

https://doi.org/10.5194/hess-15-453-2011

Mourad, R., Schoups, G., Bastiaanssen, W., & Kumar, D.N. (2024). Expert-based prior uncertainty analysis of gridded water balance components: Application to the irrigated Hindon River Basin, India. *Journal of Hydrology: Regional Studies, 55*, 2214-5818. https://doi.org/10.1016/j.ejrh.2024.101935.

Mueller, B., Seneviratne, S. I., Jimenez, C., Corti, T., Hirschi, M., Balsamo, G., . . . Guo, Z. (2011). Evaluation of global observations-based evapotranspiration datasets and IPCC AR4 simulations. *Geophysical Research Letters, 38*(6). https://doi.org/10.1029/2010GL046230

Munier, S., & Aires, F. (2018). A new global method of satellite dataset merging and quality characterization constrained by the terrestrial water budget. *Remote Sensing of Environment, 205*, 119-130. https://doi.org/10.1016/j.rse.2017.11.008

Pan, M., Sahoo, A. K., Troy, T. J., Vinukollu, R. K., Sheffield, J., & Wood, E. F. (2012). Multisource estimation of long-term terrestrial water budget for major global river basins. *Journal of Climate, 25*(9), 3191-3206. https://doi.org/10.1175/JCLI-D-11-00300.1

Pan, S., Pan, N., Tian, H., Friedlingstein, P., Sitch, S., Shi, H., . . . Kato, E. (2020). Evaluation of global terrestrial evapotranspiration using state-of-the-art approaches in remote sensing, machine learning and land surface modeling. *Hydrology and Earth System Sciences, 24*(3), 1485-1509. https://doi.org/10.5194/hess-24-1485-2020

https://doi.org/10.5194/egusphere-2025-990
Preprint. Discussion started: 22 April 2025

Papacharalampous, G., Tyralis, H., Markonis, Y., Máca, P., & Hanel, M. (2023). Features of the Earth's seasonal hydroclimate: characterizations and comparisons across the Köppen–Geiger climates and across continents. *Progress in Earth and Planetary Science, 10*(1), 46. https://doi.org/10.1186/s40645-023-00574-y

Park, J., & Choi, M. (2015). Estimation of evapotranspiration from ground-based meteorological data and global land data assimilation system (GLDAS). *Stochastic Environmental Research and Risk Assessment, 29*, 1963-1992. https://doi.org/10.1007/s00477-014-1004-2

Rodell, M., Velicogna, I., & Famiglietti, J. S. (2009). Satellite-based estimates of groundwater depletion in India. *Nature, 460*(7258), 999-1002. https://doi.org/10.1038/nature08238

Schneider, U., Fuchs, T., Meyer-Christoffer, A., & Rudolf, B. (2008). Global precipitation analysis products of the GPCC. *Global Precipitation Climatology Centre (GPCC), DWD, Internet Publikation, 112*, 3819-3837.

Su, Y., & Zhang, S. (2024). Optimizing Parameters in the Common Land Model by Using Gravity Recovery and Climate Experiment Satellite Observations. *Land, 13*(4), 508. https://doi.org/10.3390/land13040508

Tapley, B. D., Bettadpur, S., Ries, J. C., Thompson, P. F., & Watkins, M. M. (2004). GRACE measurements of mass variability in the Earth system. *science, 305*(5683), 503-505. https://dor.org/10.1126/science.1099192

Watkins, M. M., Wiese, D. N., Yuan, D. N., Boening, C., & Landerer, F. W. (2015).

https://doi.org/10.5194/egusphere-2025-990
Preprint. Discussion started: 22 April 2025

Improved methods for observing Earth's time variable mass distribution with GRACE using spherical cap mascons. *Journal of Geophysical Research: Solid Earth, 120*(4), 2648-2671. https://doi.org/10.1002/2014JB011547

Wong, J. S., Zhang, X., Gharari, S., Shrestha, R. R., Wheater, H. S., & Famiglietti, J. S. (2021). Assessing water balance closure using multiple data assimilation– and remote sensing–based datasets for canada. *Journal of Hydrometeorology, 22*(6), 1569-1589. https://doi.org/10.1175/JHM-D-20-0131.1

Xu, T., Guo, Z., Xia, Y., Ferreira, V. G., Liu, S., Wang, K., . . . Zhao, C. (2019). Evaluation of twelve evapotranspiration products from machine learning, remote sensing and land surface models over conterminous United States. *Journal of Hydrology, 578*, 124105. https://doi.org/10.1016/j.jhydrol.2019.124105

Yao, Y., Liang, S., Li, X., Hong, Y., Fisher, J. B., Zhang, N., . . . Zhang, X. (2014). Bayesian multimodel estimation of global terrestrial latent heat flux from eddy covariance, meteorological, and satellite observations. *Journal of Geophysical Research: Atmospheres, 119*(8), 4521-4545. https://doi.org/10.1002/2013JD020864

Yeh, P. J. F., Swenson, S. C., Famiglietti, J. S., & Rodell, M. (2006). Remote sensing of groundwater storage changes in Illinois using the Gravity Recovery and Climate Experiment (GRACE). *Water Resources Research, 42*(12). https://doi.org/10.1029/2006WR005374

Zhang, Y., Pan, M., Sheffield, J., Siemann, A. L., Fisher, C. K., Liang, M., . . . Houser,

https://doi.org/10.5194/egusphere-2025-990
Preprint. Discussion started: 22 April 2025

P. R. (2018). A Climate Data Record (CDR) for the global terrestrial water budget: 1984–2010. *Hydrology and Earth System Sciences, 22*(1), 241-263. https://doi.org/10.5194/hess-22-241-2018

Zheng, X., Liu, D., Huang, S., Wang, H., & Meng, X. (2025). Achieving water budget closure through physical hydrological process modelling: Insights from a large-sample study. *Hydrology and Earth System Sciences*, *29*(3), 627-653. https://doi.org/10.5194/hess-29-627-2025

Zhou, L., Cao, Y., Shi, C., Liang, H., & Fan, L. (2024). Quantifying the Atmospheric Water Balance Closure over Mainland China Using Ground-Based, Satellite, and Reanalysis Datasets. *Atmosphere, 15*(4), 497. https://doi.org/10.3390/atmos15040497